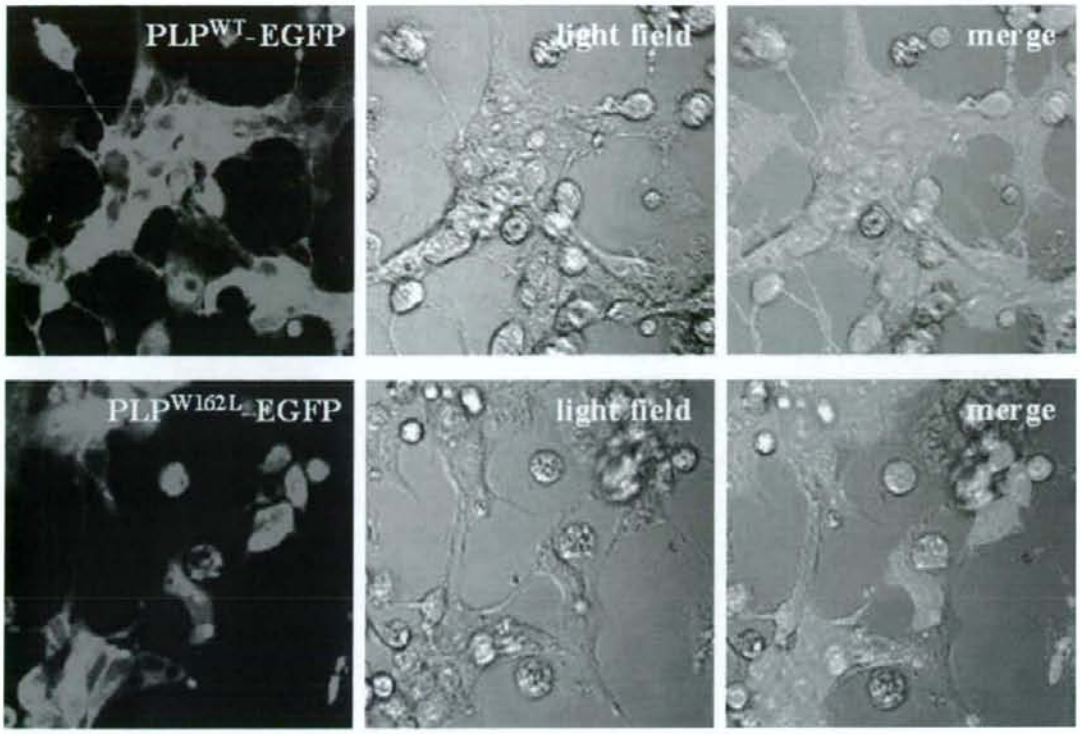

Fig. 3. Intracellular distribution of PLP^{WT}-EGFP and PLP^{W162L}-EGFP in COS-7 cells. Image of wild-type or the Trp^{162}Leu mutant PLP-EGFP visualized by laser scanning microscopy is overlaid with its light field micrograph.

was also localized to the perinuclear rim (Fig. 4D, an arrowhead and Supplement 1).

Detailed analyses of subcellular localization of PLP^{W162L}-EGFP accumulating in the perinuclear region

Following our discovery that PLP^{W162L}-EGFP expressed in COS-7 cells does not colocalize with an ER marker but accumulates at the perinuclear rim (Fig. 2D, arrows), we suspected that the Trp^{162}Leu mutant localizes to the NE. The NE was recently proposed to be a site of action of torsinA mutants, resulting in a CNS disorder known as torsion dystonia type 1 (DYT1 dystonia) (Gonzalez-Alegre and Paulson, 2004; Goodchild and Dauer, 2004; Naismith et al., 2004). Thus, we next tested whether the Trp^{162}Leu mutant resides in the NE by immunostaining COS-7 cells with an antibody against the NE protein, laminA, 40 h after transient transfection. Immunofluorescence revealed that the Trp^{162}Leu mutant accumulating at the perinuclear rim colocalizes with laminA in many cells (Fig. 5A, arrows and Supplement 2), suggesting that PLP^{W162L}-EGFP concentrates in the NE. By contrast, neither PLP^{WT}-EGFP (Fig. 5B) nor PLP^{msd}-EGFP (Fig. 5C) accumulated in the NE in most cells, although weak yellow fluorescence due to NE colocalization was occasionally seen (Fig. 5B and C, arrows). These results are consistent with the previously reported immunofluorescence studies showing that proteins retained in the ER, such as wild-type torsinA, have some colocalization with the NE (Gonzalez-Alegre and Paulson, 2004; Goodchild and Dauer, 2004).

Subcellular localization of PLP^{W162L}-FLAG transiently expressed in COS-7 cells

The absence of transiently expressed PLP^{W162L}-EGFP in the ER could also possibly be due to the large, artificially linked EGFP moiety. Therefore, we tested whether PLP^{W162L} tethered to a small peptide tag (FLAG), instead of EGFP, is retained in the ER after transfection. Twenty hours or 40 h after transient transfection in COS-7 cells, PLP-FLAGs were detected by immunofluorescence staining and confocal microscopy. Grp78/BiP immunostaining was used as an ER marker. Transiently transfected PLP^{WT}-FLAG was distributed in the cytosol (Fig. 6A) and weakly colocalized with BiP (Fig. 6A, arrows), confirming that there is no significant accumulation in the ER, similar to the EGFP-fused protein. As expected, PLP^{msd}-FLAG immunofluorescence was found in the perinuclear region and overlapped with BiP (Fig. 6B). Neither PLP^{WT}-FLAG nor PLP^{msd}-FLAG accumulations were detected at the perinuclear rim (Fig. 6A and B). Some PLP^{W162L}-FLAGs were also found

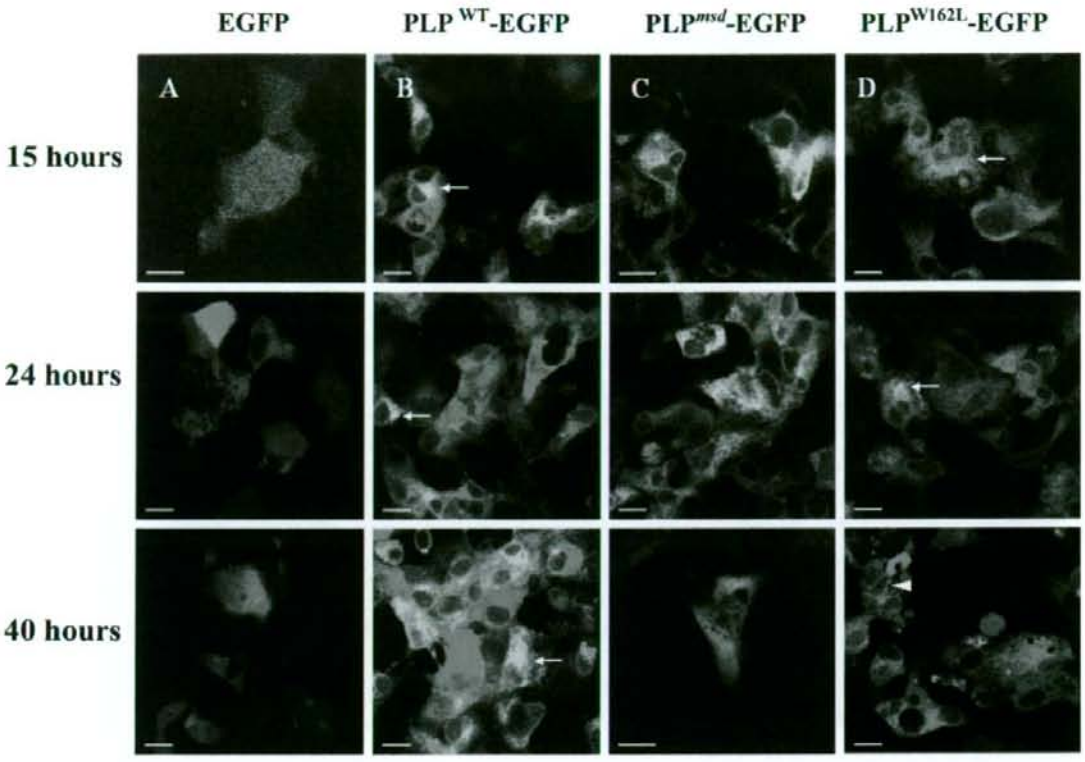

Fig. 4. Time-course monitoring of the subcellular localization of PLP-EGFPs in live cells. COS-7 cells were transiently transfected with EGFP (A), PLP^{WT}-EGFP (B), PLP^{msd}-EGFP (C), or PLP^{W162L}-EGFP (D) and visualized (green) by laser scanning microscopy. ER was simultaneously stained (red) by co-transfection of DsRed2-ER. Confocal images were collected at the indicated time points after transfection. Panels depicted are representative, single optical slices of three independent experiments. Yellow to orange color is indicative of colocalized PLP-EGFPs and ER. Arrows are indicative of ER localizations of wild-type or Trp^{162}Leu mutant PLP-EGFPs. The arrowhead in D is indicative of perinuclear rim localization of PLP^{W162L}-EGFP. Scale bars=20 μm.

localized in the perinuclear region and weakly colocalized with BiP (Fig. 6C, an arrow). Perinuclear rim localization of this mutant PLP was occasionally seen (Fig. 6C, inset). However, PLP^{W162L}-FLAG colocalized only partially with BiP (Fig. 6C, an arrowhead) in many cells and distributed in the cytosol similar to the wild-type PLP, indicating detachment of the Trp^{162}Leu mutant from the ER after translation. These data exclude the possibility that adding EGFP changed the subcellular localization of PLP.

DISCUSSION

The fact that the majority of *PLP1* point mutations cause more severe dysmyelinating disease than those caused by *null* mutations (i.e. deletions and truncations within exon 1) suggests that the profound dysmyelination resulting from *PLP1* point mutations and overexpressions probably arises not from absence of functional protein, but rather from the cytotoxic effect of mutant proteins. PLPs translated from the transfected *PLP1* cDNA with disease-associated point mutations are known to be trapped in the ER of glial tissue (Southwood et al., 2002) and non-glial cells (Gow et al., 1994b; Gow and Lazzarini, 1996; Thomson et al., 1997) in the process of being transported to the cell surface. It was assumed that those mutations led to misfolding of PLPs during translation in oligodendrocytes of patients. Unfolded PLPs are thought to accumulate in the ER and then are transferred to the cytosol for ER-associated protein degradation (ERAD) to prevent resulting cytotoxic effects (Kaufman, 2002; Gow and Sharma, 2003). Excessive misfolded PLPs not processed by degradation could result in the death of oligodendrocytes by UPR-mediated apoptotic mechanisms (Kaufman, 2002).

We found a novel missense mutation (485G→T, Trp^{162}Leu) in exon 4 of the *PLP1* gene of a patient suspected of having PMD. We further showed that this disease-associated mutant PLP fused to an EGFP or a FLAG tag and transfected in COS-7 cells is not retained in the ER but accumulates in the perinuclear region. The data suggest that PLP^{W162L} escapes from trapping by the quality control machinery for newly synthesized proteins in the ER. This is in contrast to the results of previous *in vitro*

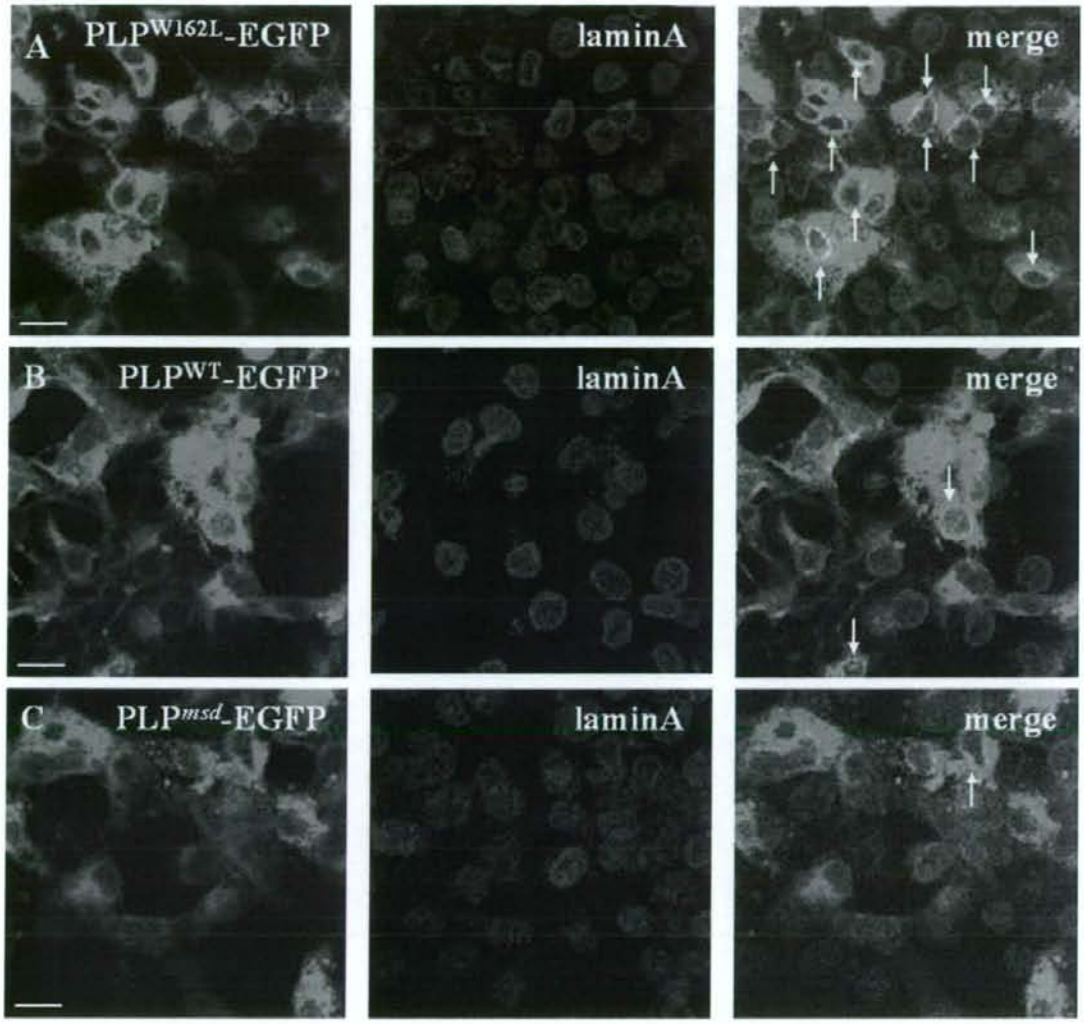

Fig. 5. Presence of PLP^{W162L}-EGFP in the NE. Forty hours after transient transfection with PLP^{W162L}-EGFP (A), PLP^{WT}-EGFP (B), or PLP^{msd}-EGFP (C), paraformaldehyde-fixed COS-7 cells were immunofluorescently stained with an antibody against the NE protein, laminA (red: Alexa 546). Yellow fluorescence is indicative of colocalized PLP^{W162L}-EGFP and NE. Panels are representative single confocal images of independent, triplicate experiments. Scale bars=20 μm.

trafficking studies showing that many transfected PLPs with naturally occurring point mutations are accumulated in the ER directly after translation (Gow et al., 1994b; Gow and Lazzarini, 1996; Thomson et al., 1997). However, it has been reported that the *partially* unfolded cystic fibrosis transmembrane conductance regulator (CFTR) protein expressed in BHK cells is not trapped in the ER whereas *fully* misfolded CFTR is retained in the ER during trafficking toward the cell surface (Sharma et al., 2004). Partially misfolded CFTR was shown to reach the cell surface but was short-lived because of degradation due to inefficient recycling at the cell surface (Gentzsch et al., 2004; Sharma et al., 2004). The lack of PLP^{W162L}-retention in the ER may be due to a similar mild alteration in its three-dimensional structure, thereby enabling it to escape from the quality control of the secretory pathway.

There was a time-dependence of the subcellular localization of PLP^{W162L}-EGFP in COS-7 cells although wild-type and *msd* mutant protein showed no such correlations. Distribution of PLP^{W162L}-EGFP in cells at early time points (15 and 24 h) after transfection (Fig. 4D) was similar to that of wild-type protein (Fig. 4B). Some observations of PLP^{W162L}-EGFPs localized in the ER were probably due to PLP molecules under translation as previously reported for wild-type PLP (Gow et al., 1994a). However, 40 h after transfection, almost no PLP^{W162L} was found localized to

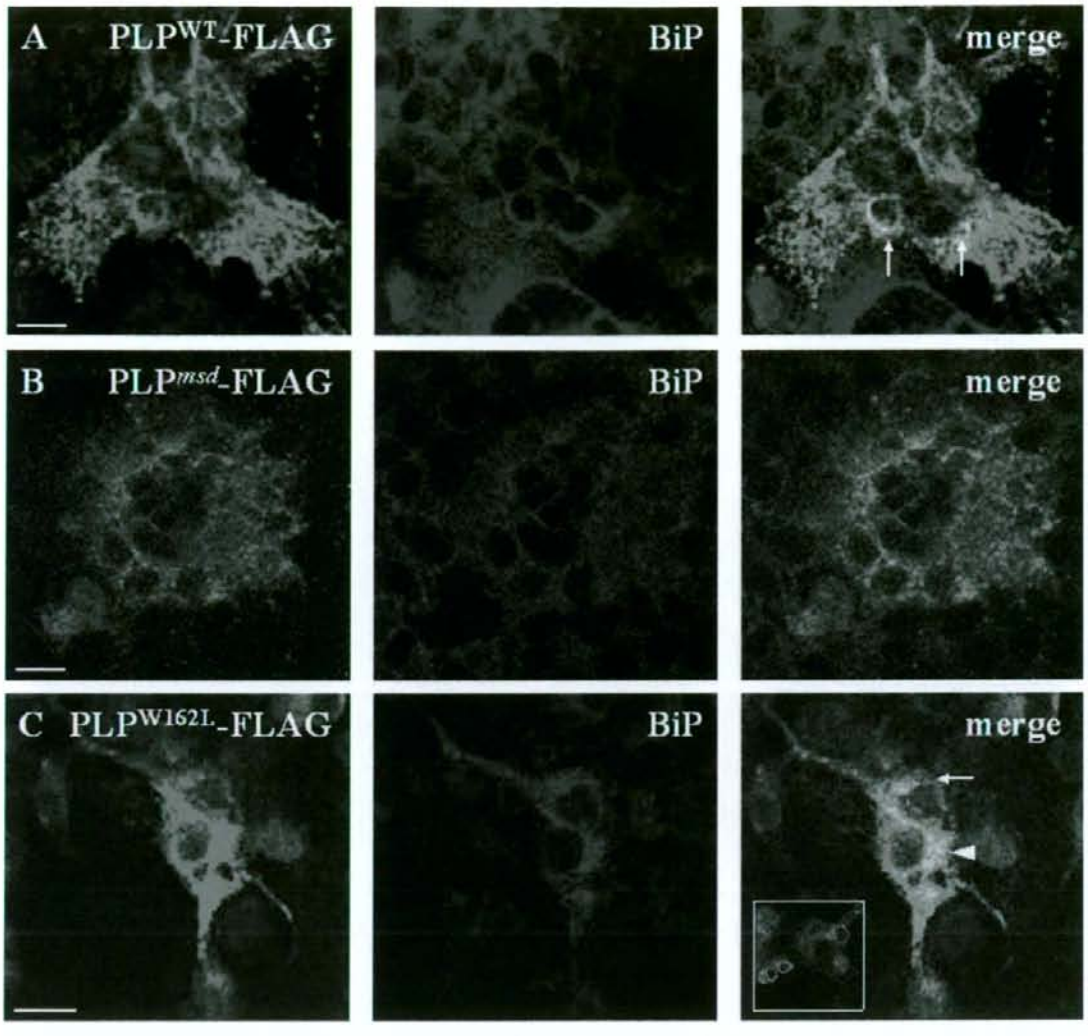

Fig. 6. Transiently transfected PLP-FLAGs in paraformaldehyde-fixed cells detected by immunofluorescence and laser scanning microscopy. COS-7 cells adhering to glass coverslips were transiently transfected with PLP^{WT}-FLAG (A), PLP^{msd}-FLAG (B), or PLP^{W162L}-FLAG (C). After 20 h of transfection, PLP-FLAGs were detected (green) by anti-FLAG immunostaining followed by Alexa 488-conjugated anti-rabbit IgG. ER was simultaneously stained (red) using a combination of anti-KDEL (BiP) antibody and Alexa 546-conjugated anti-mouse IgG. Yellow color is indicative of colocalized PLP-EGFPs and ER. Arrows in A indicate partial ER localization of PLP^{WT}-FLAG. The arrow and arrowhead in C indicate weak and partial colocalization of PLP^{W162L}-FLAG with ER, respectively. The inset in C indicates perinuclear rim localization of PLP^{W162L}-FLAG. Panels are representative, merged, single confocal images of independent triplicate experiments. Scale bars=20 μm.

the ER (Fig. 4D). We observed distinct subcellular localizations for ER and PLP^{W162L}-EGFP within most cells 40 h after transfection (Fig. 4D) and some PLP^{W162L}-EGFP was found in the NE. This is consistent with previous reports showing that accumulation of torsinA mutants at the NE is discernable from diffuse perinuclear localization of the ER (Gonzalez-Alegre and Paulson, 2004; Goodchild and Dauer, 2004). This NE-accumulation may help to explain why PLP^{W162L} does not reach the cell surface even though it passes through the ER. In this case, it is not expected that the UPR is induced. This hypothesis is consistent with the finding that the UPR is not activated by overexpression of a NE-accumulating mutant torsinA that causes DYT1 dystonia (Gonzalez-Alegre and Paulson, 2004). There may be specific quality control mechanisms for mutant proteins accumulating in the NE.

In this report, we provide evidence that a disease-associated PLP^{W162L} is not retained in the ER after translation in COS-7 cells. Absence of mutant PLP in the ER might be associated with the mild clinical symptoms

of PLP^{W162L} as is the case with PMDs associated with a null mutation of the *PLP1* gene (Raskind et al., 1991; Sistermans et al., 1996; Inoue et al., 2002). Our case supports the idea that variable PMD severity caused by missense mutations is consistent with a graded UPR from the ER. Moreover, we showed that PLP^{W162L}-EGFP unexpectedly accumulates in the NE. Aberrant subcellular distribution of mutant PLP in the NE has never been described in either PMD patients or cells transfected with mutant *PLP1* cDNA. Further, *in vivo* analyses are required to elucidate the significance of this in the pathology of PMD.

Acknowledgments—We thank K. Kikuchi for technical assistance and K. Inoue for critical review of the manuscript.

REFERENCES

Boespflug-Tanguy O, Mimault C, Melki J, Cavagna A, Giraud G, Pham Dinh D, Dastugue B, Dautigny A (1994) Genetic homogeneity of Pelizaeus-Merzbacher disease: tight linkage to the proteolipoprotein locus in 16 affected families. PMD Clinical Group. Am J Hum Genet 55:461–467.

Boucher SE, Cypher MA, Carlock LR, Skoff RP (2002) Proteolipid protein gene modulates viability and phenotype of neurons. J Neurosci 22:1772–1783.

Cerghet M, Bessert DA, Nave KA, Skoff RP (2001) Differential expression of apoptotic markers in jimpy and in Plp overexpressors: evidence for different apoptotic pathways. J Neurocytol 30:841–855.

Gentzsch M, Chang XB, Cui L, Wu Y, Ozols VV, Choudhury A, Pagano RE, Riordan JR (2004) Endocytic trafficking routes of wild type and DeltaF508 cystic fibrosis transmembrane conductance regulator. Mol Biol Cell 15:2684–2696.

Ghandour MS, Feutz AC, Jalabi W, Taleb O, Bessert D, Cypher M, Carlock L, Skoff RP (2002) Trafficking of PLP/DM20 and cAMP signaling in immortalized jimpy oligodendrocytes. Glia 40:300–311.

Gonzalez-Alegre P, Paulson HL (2004) Aberrant cellular behavior of mutant torsinA implicates nuclear envelope dysfunction in DYT1 dystonia. J Neurosci 24:2593–2601.

Goodchild RE, Dauer WT (2004) Mislocalization to the nuclear envelope: an effect of the dystonia-causing torsinA mutation. Proc Natl Acad Sci U S A 101:847–852.

Gow A (2003) The COS-7 cell in vitro paradigm to study myelin proteolipid protein 1 gene mutations. Methods Mol Biol 217:263–275.

Gow A, Friedrich VL Jr, Lazzarini RA (1994a) Intracellular transport and sorting of the oligodendrocyte transmembrane proteolipid protein. J Neurosci Res 37:563–573.

Gow A, Friedrich VL Jr, Lazzarini RA (1994b) Many naturally occurring mutations of myelin proteolipid protein impair its intracellular transport. J Neurosci Res 37:574–583.

Gow A, Lazzarini RA (1996) A cellular mechanism governing the severity of Pelizaeus-Merzbacher disease. Nat Genet 13:422–428.

Gow A, Sharma R (2003) The unfolded protein response in protein aggregating diseases. Neuromolecular Med 4:73–94.

Gow A, Southwood CM, Lazzarini RA (1998) Disrupted proteolipid protein trafficking results in oligodendrocyte apoptosis in an animal model of Pelizaeus-Merzbacher disease. J Cell Biol 140:925–934.

Griffiths I, Klugmann M, Anderson T, Thomson C, Vouyiouklis D, Nave KA (1998) Current concepts of PLP and its role in the nervous system. Microsc Res Tech 41:344–358.

Hudson LD, Puckett C, Berndt J, Chan J, Gencic S (1989) Mutation of the proteolipid protein gene PLP in a human X chromosome-linked myelin disorder. Proc Natl Acad Sci U S A 86:8128–8131.

Inoue K (2005) PLP1-related inherited dysmyelinating disorders: Pelizaeus-Merzbacher disease and spastic paraplegia type 2. Neurogenetics 6:1–16.

Inoue K, Osaka H, Thurston VC, Clarke JT, Yoneyama A, Rosenbarker L, Bird TD, Hodes ME, Shaffer LG, Lupski JR (2002) Genomic rearrangements resulting in PLP1 deletion occur by nonhomologous end joining and cause different dysmyelinating phenotypes in males and females. Am J Hum Genet 71:838–853.

Kagawa T, Ikenaka K, Inoue Y, Kuriyama S, Tsujii T, Nakao J, Nakajima K, Aruga J, Okano H, Mikoshiba K (1994) Glial cell degeneration and hypomyelination caused by overexpression of myelin proteolipid protein gene. Neuron 13:427–442.

Kaufman RJ (2002) Orchestrating the unfolded protein response in health and disease. J Clin Invest 110:1389–1398.

Naismith TV, Heuser JE, Breakefield XO, Hanson PI (2004) TorsinA in the nuclear envelope. Proc Natl Acad Sci U S A 101:7612–7617.

Osaka H, Kawanishi C, Inoue K, Onishi H, Kobayashi T, Sugiyama N, Kosaka K, Nezu A, Fujii K, Sugita K, Kodama K, Murayama K, Murayama S, Kanazawa I, Kimura S (1999) Pelizaeus-Merzbacher disease: three novel mutations and implication for locus heterogeneity. Ann Neurol 45:59–64.

Raskind WH, Williams CA, Hudson LD, Bird TD (1991) Complete deletion of the proteolipid protein gene (PLP) in a family with X-linked Pelizaeus-Merzbacher disease. Am J Hum Genet 49: 1355–1360.

Readhead C, Schneider A, Griffiths I, Nave KA (1994) Premature arrest of myelin formation in transgenic mice with increased proteolipid protein gene dosage. Neuron 12:583–595.

Roussel G, Neskovic NM, Trifilieff E, Artault JC, Nussbaum JL (1987) Arrest of proteolipid transport through the Golgi apparatus in Jimpy brain. J Neurocytol 16:195–204.

Schneider A, Montague P, Griffiths I, Fanarraga M, Kennedy P, Brophy P, Nave KA (1992) Uncoupling of hypomyelination and glial cell death by a mutation in the proteolipid protein gene. Nature 358:758–761.

Sharma M, Pampinella F, Nemes C, Benharouga M, So J, Du K, Bache KG, Papsin B, Zerangue N, Stenmark H, Lukacs GL (2004) Misfolding diverts CFTR from recycling to degradation: quality control at early endosomes. J Cell Biol 164:923–933.

Simons M, Kramer EM, Macchi P, Rathke-Hartlieb S, Trotter J, Nave KA, Schulz JB (2002) Overexpression of the myelin proteolipid protein leads to accumulation of cholesterol and proteolipid protein in endosomes/lysosomes: implications for Pelizaeus-Merzbacher disease. J Cell Biol 157:327–336.

Sistermans EA, de Wijs IJ, de Coo RF, Smit LM, Menko FH, van Oost BA (1996) A (G-to-A) mutation in the initiation codon of the proteolipid protein gene causing a relatively mild form of Pelizaeus-Merzbacher disease in a Dutch family. Hum Genet 97:337–339.

Southwood CM, Garbern J, Jiang W, Gow A (2002) The unfolded protein response modulates disease severity in Pelizaeus-Merzbacher disease. Neuron 36:585–596.

Thomson CE, Montague P, Jung M, Nave KA, Griffiths IR (1997) Phenotypic severity of murine Plp mutants reflects in vivo and in vitro variations in transport of PLP isoproteins. Glia 20:322–332.

APPENDIX

Supplementary data

Supplementary data associated with this article can be found, in the online version, at doi: 10.1016/j.neuroscience.2006.05.067.

(Accepted 22 May 2006)
(Available online 14 July 2006)

Human Molecular Genetics, 2007, Vol. 16, No. 24 **3037–3046**
doi:10.1093/hmg/ddm262
Advance Access published on September 13, 2007

Translation of *SOX10* 3′ untranslated region causes a complex severe neurocristopathy by generation of a deleterious functional domain

Ken Inoue[1,2,*], Tomoko Ohyama[2], Yosuke Sakuragi[1], Ryoko Yamamoto[1], Naoko A. Inoue[1], Yu Li-Hua[1], Yu-ichi Goto[1], Michael Wegner[3] and James R. Lupski[2,4,5]

[1]Department of Mental Retardation and Birth Defect Research, National Institute of Neuroscience, National Center of Neurology and Psychiatry, Tokyo 187-8502, Japan, [2]Department of Molecular and Human Genetics, [3]Institut für Biochemie, Emil-Fischer-Zentrum, Universität Erlangen, Erlangen D-91054, Germany, [4]Department of Pediatrics, Baylor College of Medicine and [5]Texas Children's Hospital, Houston 77030, TX

Received June 11, 2007; Revised and Accepted September 7, 2007

Peripheral demyelinating neuropathy, central dysmyelinating leukodystrophy, Waardenburg syndrome and Hirschsprung disease (PCWH) is a complex neurocristopathy caused by *SOX10* mutations. Most PCWH-associated *SOX10* mutations result in premature termination codons (PTCs), for which the molecular mechanism has recently been delineated. However, the first mutation reported to cause PCWH was a disruption of the native stop codon that by conceptual translation extends the protein into the 3′ untranslated region (3′-UTR) for an additional 82 residues. In this study, we sought to determine the currently unknown molecular pathology for the SOX10 extension mutation using *in vitro* functional assays. Despite the wild-type SOX10 coding sequence remaining intact, the extension mutation led to severely diminished transcription and DNA-binding activities. Nevertheless, it showed no dominant-negative interference with wild-type SOX10 *in vitro*. Within the 82-amino acid tail, an 11-amino acid region (termed the WR domain) was responsible primarily for the deleterious properties of the extension. The WR domain, presumably forming an α-helix structure, inhibited SOX10 transcription activities if inserted in the carboxyl-terminal half of the protein. The WR domain can also affect other transcription factors with a graded effect when fused to the carboxyl termini, suggesting that it probably elicits a toxic functional activity. Together, molecular pathology for the *SOX10* extension mutation is distinct from that of more common PTC mutations. Failure to properly terminate *SOX10* translation causes the generation of a deleterious functional domain that occurs because of translation of the normal 3′-UTR; the mutant fusion protein causes a severe neurological disease.

INTRODUCTION

Mutations in the *SOX10* gene, encoding a transcription factor, that is essential for neural crest development and myelin formation both in the central and peripheral nervous systems (CNS and PNS) (1), are associated with two distinct 'neurocristopathies'. A milder more restricted spectrum trait, Waardenburg–Hirschsprung disease (WS4, OMIM: 277580) combines Waardenburg syndrome and Hirschsprung disease (2), whereas a more severe and complex neurological trait, peripheral demyelinating neuropathy, central dysmyelinating leukodystrophy, Waardenburg syndrome and Hirschsprung disease (PCWH, OMIM: 609136) reveals additional de-/dysmyelinating phenotypes in the PNS and CNS (3–7). The vast majority of disease-associated *SOX10* mutations result in premature termination codons (PTCs), causing either WS4 or PCWH depending on the position of the mutations. The exon position of the PTC is directly associated with a sensitivity or resistance to mRNA degradation by nonsense-mediated mRNA decay (NMD) (3). Functional analyses

*To whom correspondence should be addressed at: Department of Mental Retardation and Birth Defect Research, National Institute of Neuroscience, National Center of Neurology and Psychiatry, 4-1-1 Ogawahigashi-cho, Kodaira, Tokyo 187-8502, Japan. Tel: +81-42-346-1713; Fax: +81- 42-346-1743; Email: kinoue@ncnp.go.jp

indicated that WS4 resulted from *SOX10* haploinsufficiency because the WS4-associated mutant *SOX10* mRNAs contain PTCs in the upstream exons that are subject to rapid degradation by activating the NMD surveillance pathway. In contrast, PCWH is caused by dominant-negative *SOX10* alleles because NMD is unable to detect PCWH-associated mutant mRNAs typically carrying PTCs in the last exon, thereby allowing stable translation of truncated proteins that can interfere with the wild-type SOX10 protein.

However, the first *SOX10* mutation found in a PCWH patient did not result in a PTC. It was a 12 bp deletion (designated as 1400del12) that only disrupted the normal stop codon, presumably leading to an extended in-frame translation into the 3′ untranslated region (3′-UTR) (5). As a result, an additional 82 amino acids are attached to the carboxyl terminus of the normal SOX10 protein creating a mutant fusion protein. Because of the severe neurological phenotype (i.e. PCWH) associated with this extension mutation, it is unlikely that the extension simply causes a loss-of-function allele. However, the exact molecular pathoetiology for this extension mutation remains unknown. Here, we examined the functional properties of the 1400del12 extension mutant by *in vitro* functional assays. Within this extension tail, we identified an 11 amino acid region, that is responsible for the pathologic properties of the mutant protein; i.e. dramatically diminished SOX10 DNA-binding and transcription activities. Furthermore, this domain probably forms an α-helical functional unit and also diminishes transcription activity of SOX9 and SOX11 with a graded effect. In summary, our findings suggest that the extension mutation conveys the severe neurological phenotype by a pathologic function, that is, distinct from PTC mutations, possibly mediated by a gain-of-function effect.

RESULTS

The extension mutant affects SOX10 transcription activities

We previously hypothesized that the proline-rich region within the 82-amino acid extension tail may confer an additional function to the adjacent transactivation domain (5). We surmised that proline may change the native protein structural conformation and the proline-rich region of the SOX10 extension has a moderate homology to one of the proline-rich domains of Wilms tumor 1 transcription factor, a potent transcriptional repression domain (5). We thus tested this hypothesis using *SOX10* expression plasmids carrying the 82-amino acids extension (S mutant, pCMV.SOX10.S) and an extension lacking 19 residues of proline-rich region (D mutant, pCMV.SOX10.D) (Figures 1B and 6).

First, we determined the subcellular localization of these extension mutant proteins by immunocytochemistry using Cos7 cells transiently transfected with *SOX10* expression plasmids (Fig. 1A). Similar to the wild-type and truncated Q250X SOX10 proteins, both of which predominantly localized to the nucleus, SOX10 protein with either the S or D extension is present in the nucleus. In the SOX10 protein, two nuclear localization signals (NLSs) are present flanking the high mobility group (HMG) domain (8). SOX10 also contains one nuclear export signal (NES) within the HMG domain (8). Although SOX10 normally shuttles between the nucleus and the cytoplasm, it is predominantly observed in the nucleus, because the rate of import probably exceeds the rate of export (8). In agreement with the fact that the NLS and NES are maintained in all mutants examined in this study, the extension mutants localized to the nucleus, suggesting that the extensions did not affect the subcellular localization.

Next, we determined whether the extension tail can affect the SOX10 transcription activity by luciferase reporter assays. Wild-type and mutant *SOX10* expression plasmids were transiently transfected into U138 human glioblastoma cells with a luciferase reporter plasmid containing either a synthetic SOX-responsive minimal promoter (3xSXluc) (9) or the human *GJB1* promoter (pGL3-GJB1) (10), that is, directly regulated by *SOX10*. In comparison to the wild type, transcriptional activity of the S extension mutant was dramatically diminished regardless of the promoter utilized to drive expression of the reporter (Fig. 1C showing results for *GJB1* promoter; Data for minimal promoter were not shown), suggesting that the extension completely inactivated the SOX10 transcriptional activity. Interestingly, removal of the proline-rich region from the extension tail did not restore the transcriptional activity, indicating that, contrary to our initial prediction, this proline chain is dispensable for the pathological nature of the extension.

We then examined whether the extension affects the DNA-binding capability of SOX10 protein by electrophoretic mobility shift assay (EMSA). Surprisingly, both S and D extension clones dramatically diminished the DNA-binding ability, despite the fact that the DNA-binding domain is located physically far from the extension in the primary sequence (Fig. 1D). These findings suggest that the extension may involve complex pathologic mechanisms including a major change in structural conformation.

SOX10 harbors a transactivation domain at the carboxyl terminus, that is essential for its transcriptional activity (11). Because the extension tail is located adjacent to the transactivation domain, we examined if the extension can affect the transactivation capability directly and independently. We isolated the carboxyl-terminal region of *SOX10* with extension from the HMG DNA-binding domain and amino-terminal side of the SOX10 protein, and fused it to a POU DNA-binding motif of mouse POU3F1, that is essential for DNA binding and nuclear localization, but not for transcriptional activation (12). In contrast to the prominent activation of over 15-fold by the wild-type SOX10/POU chimera (POU.C354), no activation was observed for fusion constructs with the extension tail (POU.S and POU.D), regardless of the presence or absence of the proline-rich chain (Fig. 1E). These findings suggest that the extension tail also diminishes the transactivation ability of SOX10. These results reveal that the extension mutant dramatically affects SOX10 transcriptional activity, DNA-binding ability and transactivation activity.

Identification of the critical region for the toxicity of the extension

We sought to determine if the pathogenic function of the extension mutant is conveyed by a specific protein sequence motif with functional properties, or is non-specifically determined

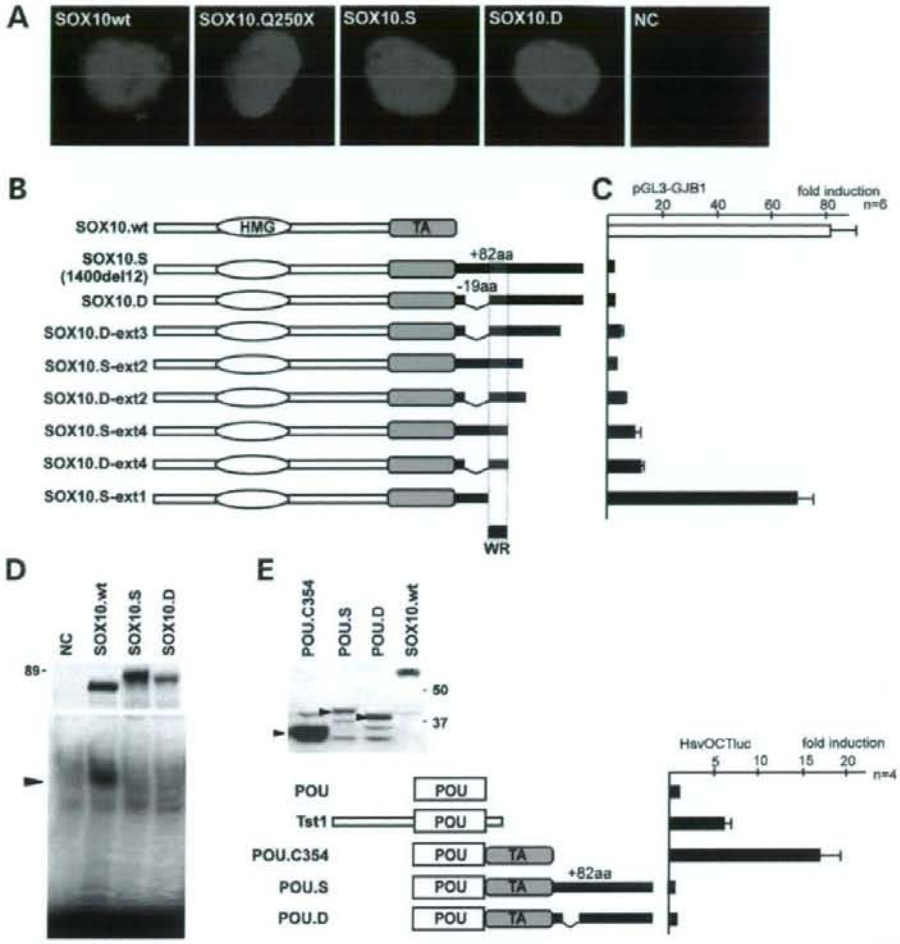

Figure 1. Subcellular localization (**A**) and *in vitro* functional assays (**B**–**E**) of SOX10 extension mutants. (A) Immunocytochemistry using SOX10 antibody shows nuclear localization of wild type, truncated mutant (Q250X), and extension mutant (S and D) SOX10 proteins. An empty vector (pCMV5) was used as a negative control (NC). (B) SOX10 extension mutants used in the assays. Filled bars at the C terminus indicate various lengths of extensions. Black rectangle below and light shade over each clone indicate the position of the WR domain. HMG, high mobility group DNA-binding domain; TA, transactivation domain. (C) Transcription activities determined by luciferase reporter assays. The luciferase reporter plasmid pGL3-GJB1 was used. The *y*-axis corresponds to the clones in (B); the *x*-axis shows the luciferase activities as the relative induction above the mean activity from transfections with luciferase reporter and empty expression plasmid, which was arbitrarily set at 1. (D) DNA-binding assay. SOX10 proteins in nuclear extracts from HeLa cells transfected with wild type (wt) or mutant SOX10 expression plasmids, shown in the western blot (top), were utilized for EMSA (bottom). As a negative control (NC), HeLa cells transfected with an empty vector (pCMV5) was used. SOX10 monomer-binding probe from *MPZ* was used. A molecular weight marker 89 kDa is shown on left. An arrowhead indicates specific binding to the target DNA. (E) Transcription activities determined by luciferase reporter assays using POU/SOX10 fusion plasmids, listed on left, and HsvOCTluc reporter plasmid. Expression of each plasmid was confirmed by western blotting using HeLa cell extract and anti-SOX10 antibody, as shown on top (arrowheads indicate specific signals, and size markers for 37 and 50 kDa are shown on right). The *x*-axis shows the luciferase activities as the relative induction above the mean activity from transfections with luciferase reporter and empty expression plasmid, which was set at 1. In (C) and (E), bars indicate mean ± s.d.

by the physical length of extension and not dependant on particular protein sequences. We generated a series of carboxyl-terminal deletions based on S and D clones, as shown in Fig. 1B, and examined their transcriptional activities by luciferase reporter assays. Among these six deletion clones, only S-ext1, which carries a 23 amino acid extension including the proline-rich region, revealed full transcriptional activity, again showing that the proline-rich region is not responsible for pathogenicity (Fig. 1C). Meanwhile, the other five clones similarly resulted in a large reduction of activity. Although there was a slight tendency for transcriptional activities to inversely increase with a decrease in length of the extension from S to D-ext4 clones, the major change in the activity (>6-fold) from D-ext4 (15 amino acid extension) to S-ext1 (23 amino acid extension) was not likely associated with the difference in the length of the extension.

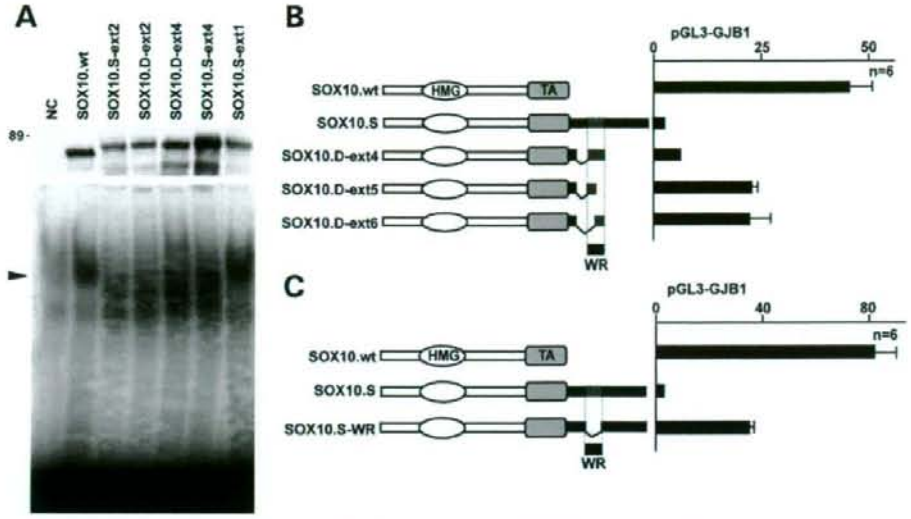

Figure 2. Functional determination of the WR domain. (**A**) DNA-binding assay using SOX10 proteins with different length of extension. SOX10 proteins in nuclear extracts from HeLa cells transfected with wild type (wt) or mutant SOX10 expression plasmids (listed in Fig 1B), shown in the western blot (top), were utilized for EMSA (bottom). As a negative control (NC), HeLa cells transfected with an empty vector (pCMV5) was used. High-affinity SOX10 monomer-binding probe from *MPZ* was used. A molecular weight marker 89 kDa is shown on left. An arrowhead indicates specific binding to the target DNA. (**B** and **C**) Transcription activities determined by luciferase reporter assays using SOX10 extension plasmids, listed on left, and pGL3-GJB1 reporter plasmid. Filled bars at the C terminus indicate various lengths of extensions. Black rectangle below and light shade over each clone indicate the position of the WR domain. HMG, high mobility group DNA-binding domain; TA, transactivation domain. The *x*-axis shows the luciferase activities as the relative induction above the mean activity from transfections with luciferase reporter and empty expression plasmid, which was arbitrarily set as 1. In (B) and (C), bars indicate mean ± s.d.

Comparison of the contents of each clone revealed that the presence of an 11 amino acid region is likely sufficient to diminish the transcriptional activity. The 11 amino acid region consists of WWWQWRRLRRL, enriched by tryptophan in the first half and by arginine in the latter half, thus we designated it as a 'WR domain' (Fig. 1B). EMSA using five of these clones showed that extension mutants with diminished transcriptional activity had defective DNA-binding ability, whereas the S-ext1 clone retained adequate DNA-binding affinity (Fig. 2A), suggesting that the WR domain is sufficient to diminish the DNA binding of the extension mutants.

To further characterize the WR domain, we determined if this 11 amino acid domain can be minimized to a smaller functional unit and yet retain pathogenicity. We removed each half of this domain from the D-ext1 clone, resulting in D-ext5 (carrying WWWQW) and D-ext6 (carrying RRLRRL), respectively (Fig. 2B). Both constructs resulted in a transcriptional up-regulation of 3-fold compared with D-ext4, leading to a restoration of transcriptional activity to half the wild type. These findings suggested that the 11 amino acids probably forms a minimal functional unit to effectively elicit the transcriptional toxicity. Furthermore, elimination of the WR domain from the S extension (designated as S-WR, Fig. 2C) up-regulated the activity by 10-fold, effectively restoring the transcriptional activity to half the wild type. These findings indicated that the WR domain is critical to the toxic function of the extension mutant, although the rest of the extension excluding the WR domain can also suppress the SOX10 activity to some extent.

Inhibitory effect of the inserted WR domain within the SOX10 protein

To determine if the toxicity of the WR domain is position-specific, we inserted this WR domain into various positions of the SOX10 protein (Fig. 3A). These positions were selected so as not to disrupt either the HMG or transactivation domains of SOX10. As controls, we inserted a 10 amino acid myc tag (EQKLISEEDL) at the same positions. Luciferase reporter assays using the *GJB1* reporter revealed that the WR domain, but not the myc tag, diminished the SOX10 transcriptional activity when it was placed downstream of the HMG domain (Fig. 3B). Data obtained using the minimal promoter (3xSXluc) conveyed similar results (data not shown). The inhibitory effect was strong at the *Nae*I and *Dra*III sites and modest at the *Pst*I site. Because, insertion of the myc tag at the same positions did not reduce the transcriptional activity, the inhibitory effect of the WR domain insertion is likely specific to its sequence content. In contrast, both the WR and myc insertions at the *Nar*I site upstream of the HMG domain conveyed an inhibitory effect, wherein the WR insertion showed a milder inhibition. This inhibition by myc insertion at the *Nar*I site was not observed when the minimal promoter was used (data not shown), suggesting that the effect of the insertions at this position may be different among different promoters.

Accordingly, EMSA showed that the WR domain insertions, but not the myc insertions, in the carboxyl-terminal half of the protein resulted in a diminished DNA-binding ability (Fig. 3C), suggesting that the WR domain specifically

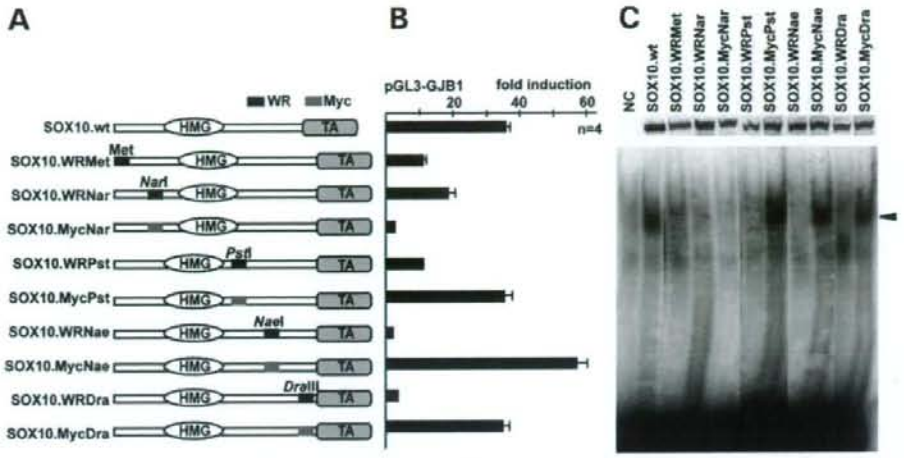

Figure 3. Functional analyses of WR domain insertions. (**A**) SOX10 mutants used in the assays. Black rectangles indicate the WR domain insertions whereas grey rectangles indicate the myc tag insertions. Positions of insertion are shown as initial methionine (Met) and restriction enzyme recognition sites (*Nar*I, *Pst*I, *Nae*I and *Dra*III). HMG, high mobility group DNA-binding domain; TA, transactivation domain. (**B**) Transcription activities determined by luciferase reporter assays using SOX10 plasmids, listed in (A), and pGL3-GJB1 reporter plasmid. The *x*-axis shows the luciferase activities as the relative induction above the mean activity from transfections with luciferase reporter and empty expression plasmid, which was arbitrarily set as 1. Bars indicate mean ± s.d. (**C**) DNA-binding assay using SOX10 proteins listed in (A). SOX10 proteins in nuclear extracts from HeLa cells transfected with wild type (wt) or mutant *SOX10* expression plasmids with either WR domain or myc insertion, shown in the western blot (top), were utilized for EMSA (bottom). As a negative control (NC), HeLa cells transfected with an empty vector (pCMV5) was used. SOX10 monomer-binding probe from *MPZ* was used. An arrowhead indicates specific binding to the target DNA.

affected the binding to the target. Insertions upstream of the HMG domain also resulted in reduced DNA-binding affinity, however, these may not be sequence specific. Because the *Nar*I insertion is located within the amino acid 61–100 region that immediately precedes the HMG domain and modulates DNA binding of SOX10 in a site-specific manner (13), the insertion may have changed the affinity to the SOX10-binding sequences present in the different probe and promoters used in the EMSA and reporter assays. Nevertheless, these findings demonstrated that the WR domain can also affect the SOX10-binding and transcriptional activities from different positions within the protein.

No dominant-negative interference with the wild-type SOX10 protein

To examine whether the SOX10 mutant proteins with extension can possibly interfere with the wild-type SOX10 protein, we performed competition assays. None of the extension mutants that harbor diminished transcription activity by itself inhibited the activity of the co-present wild-type SOX10, an observation in sharp contrast to the Q250X truncated SOX10 that elicited dominant-negative interference (Fig. 4). As predicted, S-ext1 showed an additive effect, because it retains transcription activity similar to the wild-type SOX10. These findings suggest that, at least in this experimental setting *in vitro*, extension mutants do not function as dominant-negative alleles by competing with the wild-type SOX10.

WR polypeptide inhibited SOX11, SOX9 and POU3F1 transcription activities with a graded effect

If the WR domain has a specific toxic property, it may also be able to affect other transcription factors. We thus examined the effects of the WR domain when fused to two other SOX family member proteins, SOX9 and SOX11, and to a POU domain transcription factor, POU3F1. Again, the myc tag was used as a control. Addition of the WR domain in SOX9, that belongs to the same group as SOX10 (group E), resulted in a ~70% reduction of activity on the SOX-responsive minimal reporter 3xSXluc, but only 30% reduction on the *GJB1* native promoter pGL3-GJB1 (Fig. 5A). Meanwhile, the WR domain dramatically affected SOX11, which belongs to a different subclass (group C) (1), on both minimal and *GJB1* reporters (Fig. 5B). In contrast, both myc and WR domain diminished the POU3F1 activity to one-third, thus the WR domain did not confer specific effects on POU3F1 in comparison with the addition of the myc tag (Fig. 5C). EMSA showed that, unlike SOX10, the WR domain did not confer major changes in the DNA-binding ability of SOX9, SOX11 or POU3F1. Together, the WR domain can also affect transcription factors other than SOX10 with a graded effect, being strong for SOX10 and SOX11, intermediate for SOX9 and similar to the myc tag for POU3F1. These effects may be conveyed by a toxic function of the WR domain. One should note that these findings are not readily applicable to the disease-causing mutations in *SOX9*, *SOX11* or *POU3F1*, because no naturally occurring mutations in theses genes may result in the WR domain due to the sequence divergence in their 3′-UTRs.

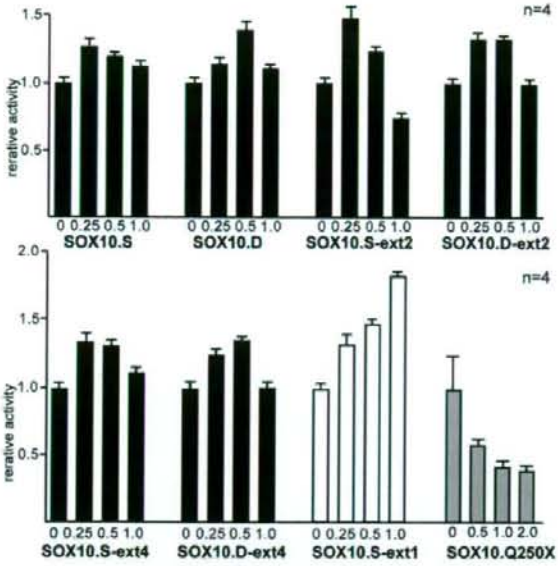

Figure 4. Competition assays. Increasing amounts of mutant *SOX10* expression plasmid were mixed with a fixed amount of wild-type *SOX10* expression plasmid and co-transfected with the luciferase reporter plasmid 3xSXluc. The *x*-axis shows the relative amount of mutant *SOX10* plasmid to the fixed wild-type *SOX10* plasmid. The total amount of DNA per well was kept constant by adding empty expression plasmid. The mean activity from transfections with the luciferase reporter and wild-type *SOX10* plasmid was set as 1, and other data are shown relative to this activity. SOX10.S-ext1 (empty bars) retains transcription activity alone, whereas six SOX10 mutants with filled bars show diminished transcription activity, as shown in Fig 1B. Nevertheless, none of the extension mutants showed dominant-negative interference as demonstrated in SOX10.Q250X truncated mutant (shaded bars). Bars indicate mean ± s.d.

Computational analyses suggest that the WR domain may form an α helix

Our findings strongly suggest that the WR domain may have functional properties that are essential for the pathologic mechanism of the extension mutant. To further delineate such properties and potentially relate them to structural features, we performed computational predictions for the extension region using various protein prediction programs, including SAM-T02 (14), through the ExPASy proteomics server (http://www.expasy.org/) (15).

Multiple secondary structural prediction analyses indicated that the WR domain may form a strong α helix structure (Fig. 6). No other region in the extension tail is predicted to form an apparent secondary structure. Examination and computational analyses of the entire extension showed two other findings: a moderate similarity to type II small proline-rich proteins identified by BLASTP and potential phosphorylation sites predicted by NetPhos (data not shown). However, the WR domain was not directly involved in these features.

DISCUSSION

In this study, we delineated the molecular pathology of a unique *SOX10* extension mutation that was found in the first PCWH patient (5) by *in vitro* functional analyses. The mutation, a 12 bp deletion starting from the second nucleotide of the native stop codon, presumably leads to a failure to properly terminate translation. As a result, by conceptual translation a putative 82-amino acid tail translated from the 3′-UTR was attached to the native carboxyl terminus of intact SOX10 protein sequence creating a mutant fusion protein (5). There is one other *SOX10* mutation with a similar extension with 86 amino acids resulting from substitution of the stop codon to lysine (X467K) (16). Although little information about the neurological examination was available for this case, the baby with this mutation showed mental and global developmental delay in addition to Waardenburg syndrome and Hirschsprung disease, suggesting that the patient probably had PCWH rather than WS4. Thus, the in-frame *SOX10* extensions are likely associated with PCWH.

Our luciferase reporter assays and EMSA demonstrated that, despite the wild-type SOX10 protein sequence remaining intact, the additive extension completely diminished the transcriptional activity both on the minimal and *GJB1* promoters, suggesting that extension may elicit deleterious effects. Because loss-of-function of one allele, or haploinsufficiency, of *SOX10* is associated with a WS4 phenotype, whereas the extension mutations cause more severe PCWH phenotype, it is unlikely that the extension mutant simply acts as a loss-of-function allele. Our competition assays demonstrated that the extension mutants do not interfere with co-present wild-type SOX10 activity, indicating that dominant-negative action is less likely, at least in our *in vitro* experimental setting. Nevertheless, these findings are not readily applicable *in vivo* without further experimental validation. Interestingly, one study reported an enhanced transcription activity of the extension mutant (1400del12) (17). We were unable to clarify the reason for this discrepancy. This study also reported reduced transcription activity for the PCWH-causing X467K mutant with an in-frame 86 amino acid extension. This latter finding is rather consistent with our results.

We found that the deleterious effect of the extension is primarily associated with a specific functional domain that plays a critical role. Within the 82-amino acid extension tail our studies using a series of deletion constructs identified an 11 amino acid region, that we termed the WR domain, to be responsible for the deleterious function. Although the WR domain polypeptide sequence does not have homology to any known proteins or functional motifs, it consists of α-helix secondary structure with high probability, which may structurally form a functional unit. Indeed, our experimental findings suggest structural effects of the WR domain. First, insertions of the WR domain at different positions specifically disrupted the DNA-binding and transcription activities only when it was placed downstream of the HMG domain. Second, WR domain attachment also affected SOX9 and SOX11 with a graded effect, but only conferred non-specific inhibition on POU3F1. Because secondary and tertiary structural predictions of the SOX10 protein revealed that the HMG DNA-binding domain is comprised of three α-helix units, while other regions appear to form no major secondary structure, we hypothesize that the α-helix WR domain may interfere with the HMG domain in a structurally specific manner. Further investigation of this currently unknown mol-

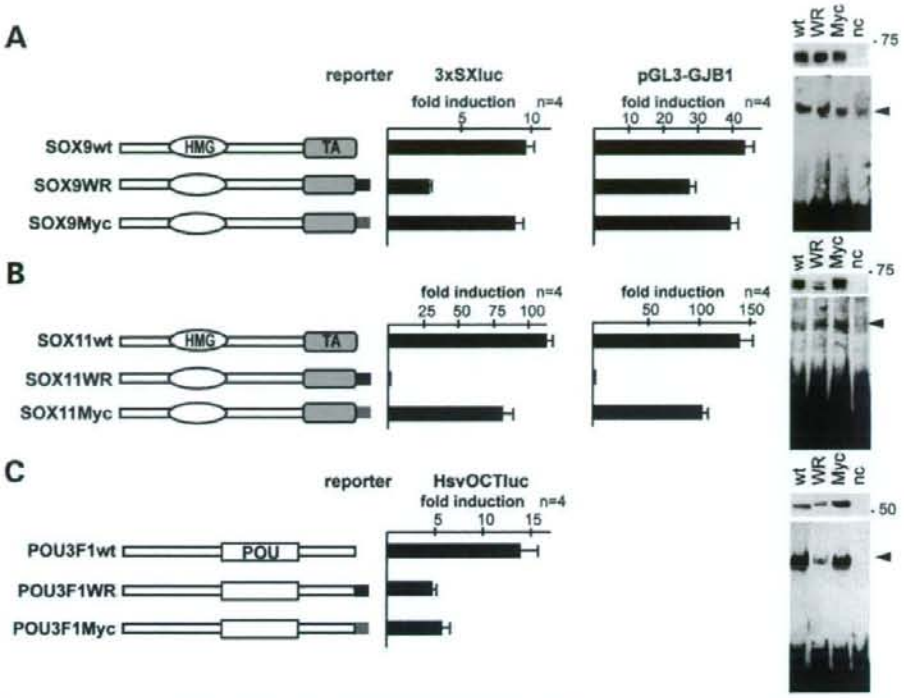

Figure 5. Inhibitory effects of the WR domain on other transcription factors. Transcription activities were determined by luciferase reporter assays using *SOX9* (**A**), *SOX11* (**B**) and *POU3F1* (**C**) plasmids, as listed on left. Black rectangles indicate the WR domain insertions whereas grey rectangles indicate the myc tag insertions. Each expression plasmid was co-transfected with either 3xSxluc (middle) or pGL3-GJB1 (right) reporter plasmid for SOX protein and HsvOCT reporter plasmid for POU3F1 protein. The *x*-axis shows the luciferase activities as the relative induction above the mean activity from transfections with luciferase reporter and empty expression plasmid, which was arbitrarily set as 1. Bars indicate mean ± s.d. DNA- binding assays and western blottings using each protein listed on left were shown on right. Protein extracts from Cos7 cells transfected with wild type (wt), WR, Myc or empty vector (negative control, nc) plasmid, shown in the western blot (top), were utilized for EMSA (bottom). SOX-binding probe was used for SOX9 and SOX11, whereas POU-binding probe was utilized for POU3F1. Molecular weight markers 75 or 50 kDa are shown on right. Arrowheads indicate specific binding to the target DNA.

ecular mechanism for the potential interaction between the WR domain and HMG domain will help clarify the pathologic basis for the toxic effect of the WR domain.

Disruption of the native stop codon without changing wild-type protein coding sequence is an uncommon cause for human genetic diseases. More frequent frame-shift mutations in the coding sequences can give rise to similar 'out-of-frame' translations, but the impact of such 'out-of-frame' tails in the disease pathoetiology probably differs case by case, depending on location of the frame-shift alteration, reading frame (i.e. one base plus or two bases plus), or actual DNA sequences comprising the coding and non-coding region of a gene, as we previously demonstrated in the myelin protein zero; *MPZ*, gene (18). In fact, at least four disease-causing frame-shift mutations have been reported in *SOX10*, namely 778delG, 795delG, 847insT and 1076delGA, resulting in 25, 19, 10 and 41 amino acid extension tails, respectively (2,3,6,19,20). Clinical severity conveyed by these mutations appears to be associated with the location of PTCs (i.e. the more proximal the truncation is located, the more severe the phenotype), but not with the length, position or protein sequence of the 'out-of-frame' tails. Of note, 1076delGA mutation, which produces the longest tail, was associated with WS4 in a family; no PCWH-associated neurological symptoms were apparent and consequently no dominant-negative interference was observed by functional assays (3). Theses findings further support the unique toxic property of the WR domain that is only conveyed by in-frame translation of the SOX10 3′-UTR.

Collectively, our *in vitro* functional analyses showed that molecular pathogenesis for PCWH caused by extension mutations is distinct from that caused by PTC mutations. We determined that the WR domain within the extension probably elicited a functional property that is responsible for the toxicity of the extension, thus causing the PCWH phenotype. Although the exact nature of this toxicity is not fully delineated yet, it probably acts through a gain-of-function mechanism.

With these findings, now the genotype–phenotype correlation of *SOX10* mutations has been consolidated. Loss-of-function alleles are associated with a milder and more restricted spectrum trait, WS4, in which no de-/dysmyelinating phenotypes in the PNS and CNS are involved. In contrast, dominant-negative alleles, mainly resulting from common

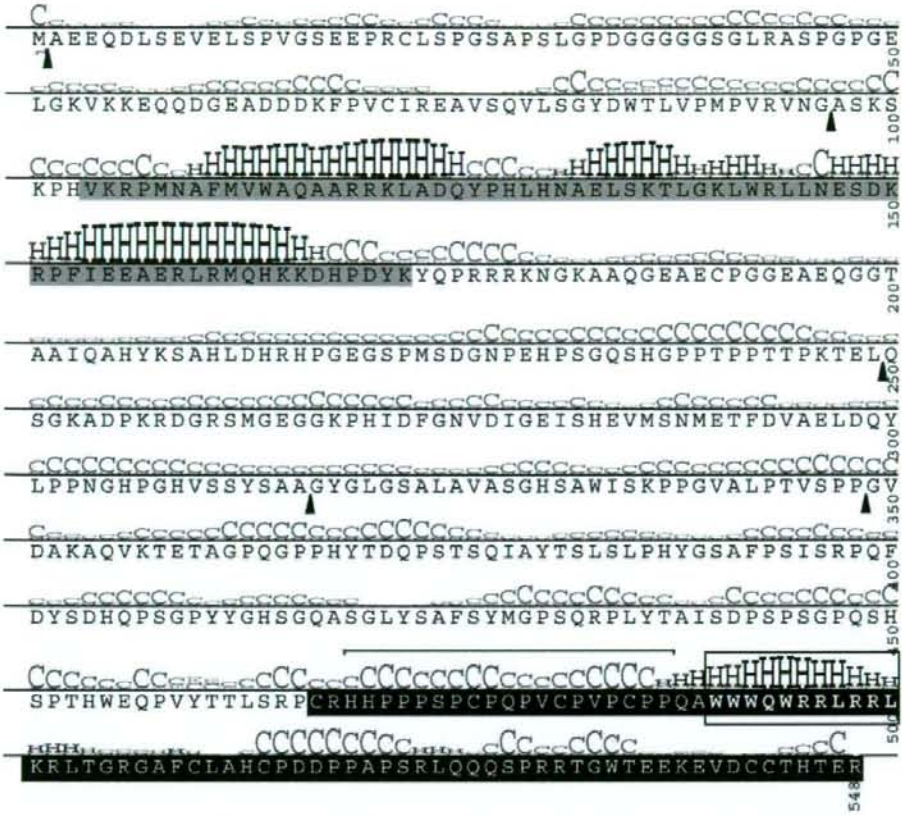

Figure 6. Predicted secondary structure of SOX10 protein with the 82-amino acid extension. Data obtained by SAM-T02 protein structure prediction program (14) are summarized. Predicted secondary structure is shown above the protein sequence for the SOX10 extension mutant. H, α helix; E, β bridges and strands; C, others including coils. The height of the letter represents the likelihood of the prediction. Shaded sequences indicate HMG domain that consists of three blocks of α helix, and the sequences written in white show the 82-amino acids extension. A rectangle indicates the WR domain, showing an α helix structure. A horizontal line indicates the proline-rich 19-amino acids region deleted in SOX10.D extension mutant. Arrowheads show the position of either WR domain or myc tag insertion indicated in Fig 3A.

PTC mutations, and gain-of-function alleles, conveyed by rare extension mutations as demonstrated in this study, give rise to more severe and complex trait, PCWH.

MATERIALS AND METHODS

Construction of expression plasmids

Human *SOX10* cDNA was inserted into a mammalian expression plasmid pCMV5 under the control of a cytomegalovirus promoter, as described (3,9). Various mutations were incorporated by PCR or PCR-based site-directed mutagenesis. Resultant mutants were: pCMV.SOX10.S that carries the 1400del12 mutation, pCMV.SOX10.D that lacks the proline-rich 19 amino acid region (HHPPPSPCPQPVCPVPCPP; see Fig. 6 for the actual location), and a 3′ end deletion series as shown in Figures 1B and 2B, designated as pCMV.SOX10.S-ext1 to pCMV.SOX10.D-ext6. The carboxyl-terminal half of *SOX10* that contains the transactivation domain was fused to a POU cassette of rat POU3F1, that contains a DNA-binding domain and nuclear localization signal, to generate pCMV.POU.C354(11), pCMV.POU.S and pCMV.POU.D (Fig. 1E). An 11 amino acid sequence (WWWQWRRLRRL; designated as the WR domain) or a myc tag (EQKLISEEDL) was inserted at various positions within the SOX10 protein (Figures 3A and 6). The WR domain was removed from pCMV.SOX10.S to generate pCMV.SOX10.S-WR (Fig. 2C). The WR domain or myc tag was inserted in frame before the stop codon of rat *SOX11*, mouse *SOX9* and mouse *POU3F1* cDNA in the pCMV5 expression plasmid to generate WR or myc fusion constructs (Fig. 5).

Immunocytochemistry

Cos7 cells were grown on chamber slides in DMEM medium supplemented with 10% fetal bovine serum (FBS) and transiently transfected with *SOX10* expression plasmids using Poly-Fect transfection reagent (Qiagen, Germany). Cells were fixed

in 4% paraformaldehyde in PBS for 5 min, then washed and permeabilized with 0.1% Tween 20 in PBS for 5 min. After twice rinsing with PBS, cells were blocked with 5% normal goat serum at room temperature for 1 h and incubated with rabbit anit-SOX10 antibody (1:500 dilution; Chemicon, CA, USA) at 4°C overnight, followed by two washes with PBS and incubation with AlexaFluor488 goat anti-rabbit antibody (1:5000: Invitrogen, CA, USA) for 1 h at room temperature before visualization by standard fluorescent microscopy. For nuclei staining, an AntiFade Kit with 4′,6′-diamidino-2-phenylindole (Invitrogen) was used.

Transfection assays using luciferase reporter system

Two SOX10-responsive luciferase reporter plasmids, 3xSXluc and pGL3-GJB1 [termed pGL3-Cx32 in our previous study (3)], and one POU-responsive reporter plasmid, HsvOCTluc, were prepared as described previously (3,9,10). U138 human glioblastoma cells were grown in DMEM medium supplemented with 10% FBS and were transiently transfected using PolyFect or Lipofectamine2000 (Invitrogen) transfection reagents. We selected U138 for these studies specifically because it does not express endogenous SOX10 protein that might interfere with transfection assays (9). A total of 0.5–0.8 μg of plasmid DNA per well was used. Typically, we used 0.2 μg reporter plasmid, 0.2 μg test plasmid and 0.1 μg inner control plasmid per well. We collected cells from 24-well trays after 48 h of transfection and assayed luciferase activity using a monolight luminometer (Pharmingen, CA, USA) or TD-20/20 luminometer (Promega, WI, USA). A β-galactosidase expression plasmid, pCMVβ (Clontech, CA, USA), or *Renilla* luciferase expression plasmid, pRT-TK (Promega), were used as a reference for transfection. Each experiment was repeated at least three times with at least four independent samples per experiment. Representative results from one experiment were shown in figures.

Western blotting and EMSA

HeLa cells were grown in DMEM medium supplemented with 10% FBS. Nuclear extract was obtained from HeLa cells after 48 h of transfection (21), which was used for western blotting and EMSA. Rabbit antibody to SOX10 (1:3000 dilution) was used for western blots. Other antibodies utilized were: goat anti-SOX9 antibody (Santa Cruz P-20, 1:500 dilution), guinea pig anti-SOX11 antibody (1:3000 dilution) (22) and goat anti-POU3F1 antibody (Santa Cruz H-13, 1:500 dilution). A 15 bp probe containing the high-affinity monomer *SOX10*-binding site found in *MPZ* gene promoter (site B) (23) or 29 bp probe containing POU-binding site (HsvOCT) (9) was used for EMSA, as described previously (3). We selected this *MPZ SOX10* monomer-binding probe, rather than *GJB1* dimer-binding site, due to its simplicity, its well-characterized property and its strong binding affinity (13,23). EMSA was performed using either ^{32}P-labeled or biotin-labeled probes.

Computational analyses

We determined structural and functional characteristics of the SOX10 mutant proteins by a series of web-based prediction programs, primarily available through the ExPASy proteomics web server (http://www.expasy.org/).

ACKNOWLEDGEMENTS

We thank Dr Chihiro Akazawa for his helpful discussions and Dr Kimiko Deguchi for her suggestions and support. This study was supported in part by following grants from the Japanese Ministry of Health, Labor, and Welfare, research grant for Nervous and Mental Disorders (19A-5), and Health and Labor Science Research Grant, Japan (H18-Kokoro-Ippan-015, KI); from the Japanese Ministry of Education, Culture, Sports, Science and Technology Grant-in-Aid for Scientific Research (17390102 to K.I.); from U.S. National Institute for Neurological Disorders and Strokes, U.S. National Institute of Health grant (RO1 NS27042 to J.R.L.).

Conflict of Interest statement. None declared.

REFERENCES

1. Wegner, M. and Stolt, C.C. (2005) From stem cells to neurons and glia: a Soxist's view of neural development. *Trends Neurosci.*, **28**, 583–588.
2. Pingault, V., Bondurand, N., Kuhlbrodt, K., Goerich, D.E., Préhu, M.O., Puliti, A., Herbarth, B., Hermans-Borgmeyer, I., Legius, E., Matthijs, G. *et al.* (1998) *SOX10* mutations in patients with Waardenburg-Hirschsprung disease. *Nat. Genet.*, **18**, 171–173.
3. Inoue, K., Khajavi, M., Ohyama, T., Hirabayashi, S., Wilson, J., Reggin, J.D., Mancias, P., Butler, I.J., Wilkinson, M.F., Wegner, M. *et al.* (2004) Molecular mechanism for distinct neurological phenotypes conveyed by allelic truncating mutations. *Nat. Genet.*, **36**, 361–369.
4. Inoue, K., Shilo, K., Boerkoel, C.F., Crowe, C., Sawady, J., Lupski, J.R. and Agamanolis, D.P. (2002) Congenital hypomyelinating neuropathy, central dysmyelination, and Waardenburg-Hirschsprung disease: phenotypes linked by *SOX10* mutation. *Ann. Neurol.*, **52**, 836–842.
5. Inoue, K., Tanabe, Y. and Lupski, J.R. (1999) Myelin deficiencies in both the central and the peripheral nervous systems associated with a *SOX10* mutation. *Ann. Neurol.*, **46**, 313–318.
6. Pingault, V., Guiochon-Mantel, A., Bondurand, N., Faure, C., Lacroix, C., Lyonnet, S., Goossens, M. and Landrieu, P. (2000) Peripheral neuropathy with hypomyelination, chronic intestinal pseudo-obstruction and deafness: a developmental 'neural crest syndrome' related to a SOX10 mutation. *Ann. Neurol.*, **48**, 671–676.
7. Touraine, R.L., Attié-Bitach, T., Manceau, E., Korsch, E., Sarda, P., Pingault, V., Encha-Razavi, F., Pelet, A., Augé, J., Nivelon-Chevallier, A. *et al.* (2000) Neurological phenotype in Waardenburg syndrome type 4 correlates with novel *SOX10* truncating mutations and expression in developing brain. *Am. J. Hum. Genet.*, **66**, 1496–1503.
8. Rehberg, S., Lischka, P., Glaser, G., Stamminger, T., Wegner, M. and Rosorius, O. (2002) Sox10 is an active nucleocytoplasmic shuttle protein, and shuttling is crucial for Sox10-mediated transactivation. *Mol. Cell. Biol.*, **22**, 5826–5834.
9. Kuhlbrodt, K., Herbarth, B., Sock, E., Hermans-Borgmeyer, I. and Wegner, M. (1998) Sox10, a novel transcriptional modulator in glial cells. *J. Neurosci.*, **18**, 237–250.
10. Bondurand, N., Girard, M., Pingault, V., Lemort, N., Dubourg, O. and Goossens, M. (2001) Human Connexin 32, a gap junction protein altered in the X-linked form of Charcot-Marie-Tooth disease, is directly regulated by the transcription factor SOX10. *Hum. Mol. Genet.*, **10**, 2783–2795.
11. Kuhlbrodt, K., Schmidt, C., Sock, E., Pingault, V., Bondurand, N., Goossens, M. and Wegner, M. (1998) Functional analysis of Sox10 mutations found in human Waardenburg-Hirschsprung patients. *J. Biol. Chem.*, **273**, 23033–23038.
12. Sock, E., Enderich, J., Rosenfeld, M.G. and Wegner, M. (1996) Identification of the nuclear localization signal of the POU domain protein Tst-1/Oct6. *J. Biol. Chem.*, **271**, 17512–17518.

13. Peirano, R.I. and Wegner, M. (2000) The glial transcription factor Sox10 binds to DNA both as monomer and dimer with different functional consequences. *Nucleic Acids Res.*, **28**, 3047–3055.
14. Karchin, R., Cline, M., Mandel-Gutfreund, Y. and Karplus, K. (2003) Hidden Markov models that use predicted local structure for fold recognition: alphabets of backbone geometry. *Proteins*, **51**, 504–514.
15. Gasteiger, E., Gattiker, A., Hoogland, C., Ivanyi, I., Appel, R.D. and Bairoch, A. (2003) ExPASy: the proteomics server for in-depth protein knowledge and analysis. *Nucleic Acids Res.*, **31**, 3784–3788.
16. Sham, M.H., Lui, V.C.L., Chen, B.L.S., Fu, M. and Tam, P.K.H. (2001) Novel mutations of *SOX10* suggest a dominant negative role in Waardenburg-Shah syndrome. *J. Med. Genet.*, **38**, E30.
17. Chan, K.K., Wong, C.K., Lui, V.C., Tam, P.K. and Sham, M.H. (2003) Analysis of *SOX10* mutations identified in Waardenburg-Hirschsprung patients: differential effects on target gene regulation. *J. Cell. Biochem.*, **90**, 573–585.
18. Khajavi, M., Inoue, K., Wiszniewski, W., Ohyama, T., Snipes, G.J. and Lupski, J.R. (2005) Curcumin treatment abrogates endoplasmic reticulum retention and aggregation-induced apoptosis associated with neuropathy-causing myelin protein zero-truncating mutants. *Am. J. Hum. Genet.*, **77**, 841–850.
19. Pingault, V., Girard, M., Bondurand, N., Dorkins, H., Van Maldergem, L., Mowat, D., Shimotake, T., Verma, I., Baumann, C. and Goossens, M. (2002) *SOX10* mutations in chronic intestinal pseudo-obstruction suggest a complex physiopathological mechanism. *Hum. Genet.*, **111**, 198–206.
20. Shimotake, T., Tanaka, S., Fukui, R., Makino, S. and Maruyama, R. (2007) Neuroglial disorders of central and peripheral nervous systems in a patient with Hirschsprung's disease carrying allelic SOX10 truncating mutation. *J. Pediatr. Surg.*, **42**, 725–731.
21. Andrews, N.C. and Faller, D.V. (1991) A rapid micropreparation technique for extraction of DNA-binding proteins from limiting numbers of mammalian cells. *Nucleic Acids Res.*, **19**, 2499.
22. Potzner, M.R., Griffel, C., Lütjen-Drecoll, E., Bösl, M.R., Wegner, M. and Sock, E. (2007) Prolonged Sox4 expression in oligodendrocytes interferes with normal myelination in the central nervous system. *Mol. Cell. Biol.*, **27**, 5316–5326.
23. Peirano, R.I., Goerich, D.E., Riethmacher, D. and Wegner, M. (2000) Protein zero gene expression is regulated by the glial transcription factor Sox10. *Mol. Cell. Biol.*, **20**, 3198–3209.

Epilepsy Research (2007) xxx, xxx–xxx

ELSEVIER

journal homepage: www.elsevier.com/locate/epilepsyres

Patients with a sodium channel alpha 1 gene mutation show wide phenotypic variation

Hitoshi Osaka[a,b,*], Ikuo Ogiwara[c], Emi Mazaki[c], Nami Okamura[c], Sumimasa Yamashita[a], Mizue Iai[a], Michiko Yamada[a], Kenji Kurosawa[d], Hiroko Iwamoto[e], Norio Yasui-Furukori[f], Sunao Kaneko[f], Tateki Fujiwara[g], Yushi Inoue[g], Kazuhiro Yamakawa[c,**]

[a] *Division of Neurology, Kanagawa Children's Medical Center, Yokohama 232-8555, Japan*
[b] *Molecular Pathology & Genetics Division, Kanagawa Cancer Center Research Institute, Yokohama 241-0815, Japan*
[c] *Laboratory for Neurogenetics, RIKEN Brain Science Institute, 2-1 Hirosawa, Wako-shi, Saitama 351-0198, Japan*
[d] *Division of Genetics, Kanagawa Children's Medical Center, Yokohama 232-8555, Japan*
[e] *Division of Pediatric Neurology, Yokohama Ryoiku Iryou Center, Yokohama 241-0014, Japan*
[f] *Department of Neuropsychiatry, School of Medicine, Hirosaki University, Hirosaki-shi, Aomori 036-8562, Japan*
[g] *National Epilepsy Center, Shizuoka Institute of Epilepsy and Neurological Disorders, Shizuoka 420-8688, Japan*

Received 19 December 2006; received in revised form 30 March 2007; accepted 31 March 2007

KEYWORDS
SCN1A;
Epilepsy;
Sodium channel

Summary We investigated the roles of mutations in voltage-gated sodium channel alpha 1 subunit gene (*SCN1A*) in epilepsies and psychiatric disorders. The *SCN1A* gene was screened for mutations in three unrelated Japanese families with generalized epilepsy with febrile seizure plus (GEFS+), febrile seizure with myoclonic seizures, or intractable childhood epilepsy with generalized tonic–clonic seizures (ICEGTC). In the family with GEFS+, one individual was affected with panic disorder and seizures, and another individual was diagnosed with Asperger syndrome and seizures. The novel mutation V1366I was found in all probands and patients with psychiatric disorders of the three families. These results suggest that *SCN1A* mutations may confer susceptibility to psychiatric disorders in addition to variable epileptic seizures. Unidentified modifiers may play critical roles in determining the ultimate phenotype of patients with sodium channel mutations.

* Corresponding author at: Division of Neurology, Kanagawa Children's Medical Center, Yokohama 232-8555, Japan. Tel.: +81 45 711 2351; fax: +81 45 721 3324.
** Corresponding author. Tel.: +81 48 467 9703; fax: +81 48 467 7095.
E-mail addresses: kcmc.ho@cameo.plala.or.jp (H. Osaka), yamakawa@brain.riken.jp (K. Yamakawa).

0920-1211/$ – see front matter © 2007 Elsevier B.V. All rights reserved.
doi:10.1016/j.eplepsyres.2007.03.018

Please cite this article in press as: Osaka, H. et al., Patients with a sodium channel alpha 1 gene mutation show wide phenotypic variation, Epilepsy Res. (2007), doi:10.1016/j.eplepsyres.2007.03.018

Introduction

Voltage-gated sodium channels (SCN) are the primary molecules responsible for generating action potentials in nervous system, skeletal and cardiac muscle, and mutations in the genes encoding those expressed in neurons including Nav1.1 encoded by *SCN1A* have been reported to cause epilepsies (Goldin, 2001).

Generalized epilepsy with febrile seizures plus (GEFS+) (OMIM604233) is dominantly inherited epilepsy characterized by febrile seizures in childhood progressing to afebrile generalized epilepsy in adults (Scheffer and Berkovic, 1997; Wallace et al., 2002). More than ten *SCN1A* missense mutations have been reported in GEFS+ families, approximately 10% of cases examined (Abou-Khalil et al., 2001; Annesi et al., 2003; Bonanni et al., 2004; Ceulemans et al., 2004; Escayg et al., 2001; Gerard et al., 2002; Ito et al., 2002; Lerche et al., 2001; Spampanato et al., 2003; Sugawara et al., 2001; Wallace et al., 2001). The penetrance is less than 80% (Scheffer and Berkovic, 1997; Singh et al., 1999; Wallace et al., 2002). In GEFS+, patients in the same pedigree express variable phenotype, febrile seizures often extending age of 6 years and afebrile generalized tonic–clonic seizures, absence, myoclonic and focal seizures (Ito et al., 2002; Scheffer and Berkovic, 1997; Singh et al., 1999).

Mutations of *SCN1A* were also identified in another epileptic syndrome; severe myoclonic epilepsy of infancy (SMEI). This disorder is characterized by early onset refractory generalized tonic–clonic or unilateral convulsions usually within the first 6 months of life, followed by additional myoclonic seizures often accompanied by mental deterioration (OMIM 182389). Some patients experience additional complex partial seizures or absence seizures. More than 150 mutations have been identified in children with this disorder, 50–80% of SMEI patients tested. Similar to GEFS+, the SMEI patients are heterozygous for the mutant alleles. Among 75 cases in which both parents have been tested, in 69 cases, or 90%, the mutations arise as *de novo* in the affected children (Meisler and Kearney, 2005; Yamakawa, 2005). Some group of patients manifest very frequent intractable GTC, usually begins in infancy, develop subsequent mental decline, as well as ataxia. They, devoid of myoclonic seizures, are proposed as intractable childhood epilepsy with generalized tonic–clonic seizures (ICEGTC). This condition has also been proven to be caused by *SCN1A* mutations (Fujiwara et al., 2003). Thus, it has been shown that the SCN mutation cause wide spectrum of febrile sensitive seizure syndromes. SMEI is the most severe phenotype within the spectrum.

In this paper, we present a novel missense mutation found in independent three families GEFS+, FS and myoclonic seizures, and ICEGTC. Members with this mutation in one of those families also showed panic disorder and Asperger syndrome. Our data suggests that the mutations of *SCN1A* provide susceptibility for psychiatric illnesses as well as fever sensitive epileptic syndromes.

Methods

Epilepsy classification

Criteria for diagnosis of SMEI were done according to the International League Against Epilepsy guidelines (1989). Patients who fulfill these criteria other than the absence of myolconic seizure were diagnosed as ICEGTC. We used the Febrile Seizures (FS) to describe with the typical febrile convulsion syndrome where all seizures occurred with fever between 3 months and 6 years. The term FS+ denotes individuals with FS and/or afebrile generalized tonic–clonic seizures (GTCS) extending beyond the age of 6 years.

Genetic analysis

We studied independent three families of GEFS+, FS and myoclonic seizures, and ICEGTC. Written informed consent was obtained from the parents or responsible adults as well as healthy control individuals where necessary and was approved by the Ethical Committees of Kanagawa Children's Medical Center, Shizuoka Medical Institute of Neurological Disorders, and the RIKEN Institute. Methods for mutational analysis of *SCN1A* were described in our previous articles (Fujiwara et al., 2003). Briefly, genomic DNA was extracted from heparin treated blood samples of affected and unaffected individuals using the QIAamp DNA Blood Midi Kit (Qiagen, Hilden, Germany) and from hair samples using the ISOHAIR Kit (Nippon Gene, Toyama, Japan). Genomic DNA was amplified by PCR with Pyrobest (TaKaRa Shuzo Co. Ltd., Tokyo, Japan) and Blend Taq Plus (Toyobo, Osaka, Japan) DNA polymerases according to the manufacturer's instructions. For mutation analysis on *SCN1A*, PCR primers were designed to amplify all 26 coding exons of *SCN1A* defined by comparison of cDNA (GenBank accession no. AY043484) and genome sequences (nos. AC010127 and AC021673). For haplotype analysis, PCR primers were designed to amplify several regions containing 8 single nucleotide polymorphism (SNP) sites in *SCN1A* (NCBI Reference SNP ID nos. rs1020852, rs2169312, rs8191987, rs994399, rs12614431, rs10497276, rs10497275 and rs2217195). PCR products were directly sequenced with a dideoxy terminator kit and analyzed by an automated sequencer (model ABI3730, Applied Biosystems, Foster City, CA).

Patients, family members, and control individuals

Family A

Patient 1 (proband, III-6; see Fig. 1A). A 9-year-old girl exhibited febrile generalized tonic–clonic convulsion at 2 years and 6 months when carbamazepine was initiated. At 3 years of age, she exhibited 1–2 times afebrile tonic convulsion. Her electroencephalograph, taken at 6 years of age, discloses normal except 4–5 Hz diffuse irregular spikes and wave complex at a drowsy state. Then valproic acid was initiated and she experienced no seizures since then. She is now the third grade of normal elementary school.

Patient 2 (III-5). This 7 years old boy, younger brother of III-6, was diagnosed as VATER association from vertebral anomaly, rectal atresia, hypoplasia of right trachea and hydrokidney. He experienced febrile generalized tonic–clonic seizure at 1 year and 2 months. Prevention for seizures by rectal diazepam was initiated since

Please cite this article in press as: Osaka, H. et al., Patients with a sodium channel alpha 1 gene mutation show wide phenotypic variation, Epilepsy Res. (2007), doi:10.1016/j.eplepsyres.2007.03.018

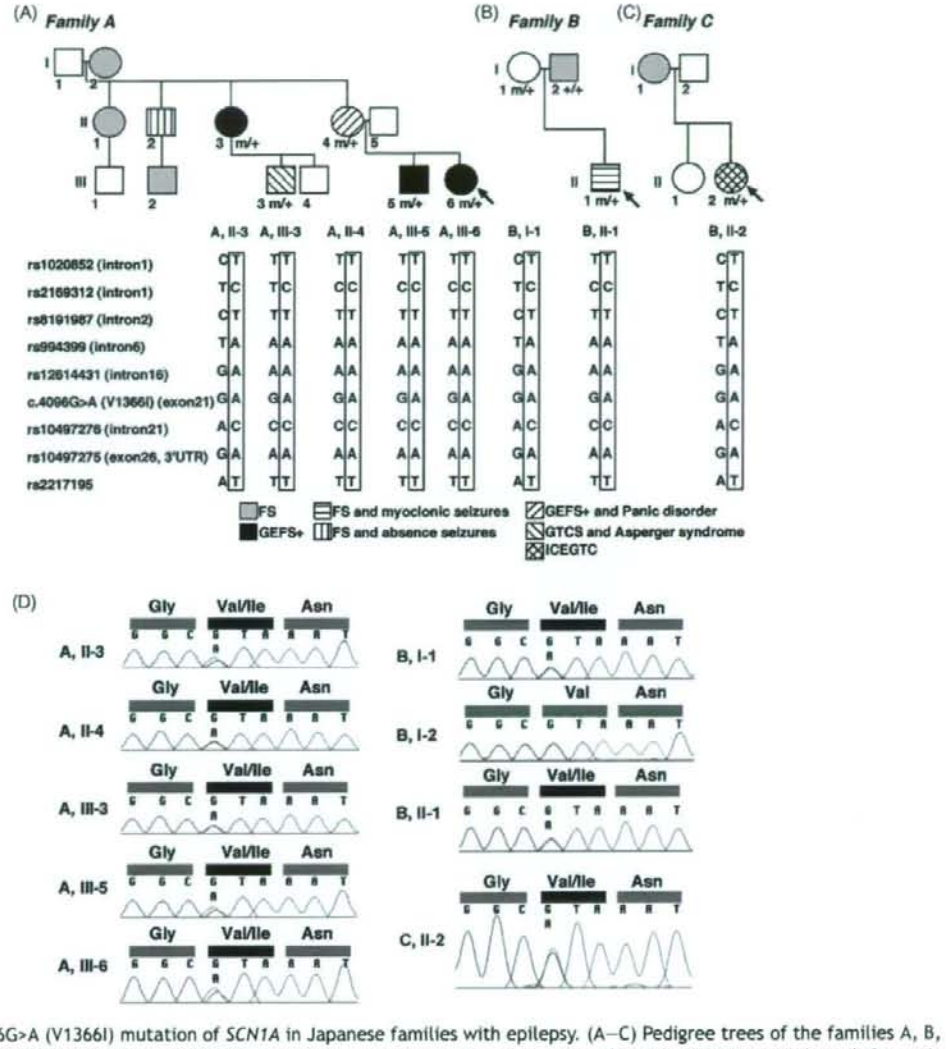

Figure 1 A c.4096G>A (V1366I) mutation of *SCN1A* in Japanese families with epilepsy. (A–C) Pedigree trees of the families A, B, and C. (m) c.4096G>A (V1366I) mutation of *SCN1A*. (+) Wild-type allele. The putative disease-associated haplotype is boxed. Genomic DNAs of members without genotypes were not available for the analysis. Circles, females; squares, males; arrows, probands. Note that members II-4 and III-3 in family A also show panic disorder and Asperger syndrome. (D) Electropherograms obtained by direct sequencings on the PCR products of *SCN1A* coding-exon 21 amplified from indicated members.

then. He exhibited afebrile absence seizures and generalized tonic–clonic seizures and valproic acid was initiated. Although Zonisamide was added for febrile seizure, he continued febrile GTC several times per year. He started to take potassium bromide at 5 years old and experienced no seizures since then. His intelligent quotient is 107 and in the second grade of normal elementary school.

Patient 3 (II-4). She is the 40-years mother of patients 1 and 2. She has febrile seizures several times until 6 yeas of ages. At her 30s, she experienced palpitation, sweating, shivering, and shortness of breathing. She was frightened the idea that she lose control of herself, make traffic accident when she drives. These symptoms worsened when she was in the crowds. She was diagnosed as having panic disorder by diagnostic criteria of DSM IV. Diazepam as anti-anxiety and paxil as anti-depressant relieve her symptoms partially and she is continuing her occupation. Her older sister (II-1) and brother (II-2) both experienced febrile seizures several times before 6 years of ages. In addition, brother (II-2) exhibited absences after 6 years of age and had valproic acid until 20 years of ages.

Patient 4 (III-3). An 8-year-old boy is maternal cousin of patients 1 and 2. He gained meaningful words at 12 months and walked alone at 16 months. He exhibited afebrile GTC at 5 years old. He had hypersensitivity to noise and explained too many anxieties. He had difficulty in social interaction

Please cite this article in press as: Osaka, H. et al., Patients with a sodium channel alpha 1 gene mutation show wide phenotypic variation, Epilepsy Res. (2007), doi:10.1016/j.eplepsyres.2007.03.018

and was reluctant to go to kindergarten. At 6 years of ages, he was diagnosed as Asperger's disorder with the diagnostic criteria of DSM-IV-TR. Pimozide relieved his violence to other students and his repetitive behavior.

Family B

Proband (II-1; see Fig. 1B). He exhibited several times of febrile GTC at 11 months. One of them lasted 25 min. EEG revealed no abnormalities. At 13 months, he experienced frequent GTC and myoclonus. Carbamazepin was initiated that was not effective for both seizures. Seizures continue more then 5 times per day. He was admitted our hospital at 21 months old. Valproate and Sodium bromide ceased seizures in 2 weeks. He is now 3 years of age. Besides one FS, he shows no seizures since then. He shows no developmental delay and neurological abnormalities. His mother (I-1) has no seizures and his father (I-2) showed one brief febrile seizure at 3 years of age.

Family C

Proband (II-2; see Fig. 1C). A 30-year-old woman had her first fever-induced GTC at age 7 months. The febrile seizure repeated monthly and from 5 years of age on she began to have afebrile GTC in addition. She once experienced convulsive status epilepticus lasting 40 min at age 5 years. The seizure was also induced by taking bath and exercise. The seizure later tended to occur in clusters a dozen to several times a day during sleep. Although her seizures had been very intractable with various medications, the seizure gradually reduced its frequency and stopped at age 20 years with the medication of valproate, phenobarbital and acetazolamide. She developed almost normally until 7 years of age. Her IQ was 50 at age 10 years and 52 at age 20 years. She showed no neurological abnormalities. She is currently visiting a sheltered workshop. The EEG showed diffuse bilateral spike-waves only when valproate was reduced, otherwise no paroxysmal discharges were recorded. MRI showed no abnormal findings. The clinical course of this patient including early onset fever-sensitive and non-sensitive refractory GTCs, paroxysms-scanty EEG and mental retardation indicates a phenotype of ICEGTC, although the seizure disappearance after 20 years of age is exceptional.

Her mother (I-1) had two febrile convulsions between the ages of 1 and 2 years, and her father (I-2) has no seizures.

Control individuals

DNAs from 304 Japanese healthy individuals were analyzed as controls in this study.

Result

We sequenced *SCN1A* gene on genomic DNAs of probands and members of families A, B, and C (Fig. 1). We identified a novel missense mutation that altered guanine at the nucleotide number at 4096 to adenine (c.4096G>A) resulting in the alteration of Valine residue at the position of 1366 in Nav1.1 into Isoleucine (V1366I) in the probands (III-6 in family A, II-1 in family B, and II-2 in family C). While this mutation was also found in other symptomatic family members (II-3, II-4, III-3, and III-5 in Family A), it was also found in an asymptomatic member (I-1 in Family B) and not found in a symptomatic member who had one febrile seizure (I-2 in Family B). This mutation was not observed in 608 alleles of Japanese healthy control individuals. Genomic DNAs of other family members were not available for the analysis, because we could not get their consent or we could not reach to the members.

We found that the V1366I mutation carriers in families A and B share a common putative SNP haplotype in the 100 kb region corresponding *SCN1A* by using 8 markers (Fig. 1A–C). Although the exact haplotype of the proband in family C were not determined because DNAs of her parents were not available for the study, she is very likely to share the same haplotype with the mutation carriers in families A and B according to the results of genotyping. Therefore, a founder effect is expected in the V1366I mutation in these three families.

Discussion

We here presented a novel *SCN1A* missense mutation, Val 1366 Ile, in three independent families of variable epilepsies including GEFS+, FS and myoclonic seizures, and ICEGTC. Putative position of aa 1366 is transmembrane domain (D3S5) of the Nav1.1 channel. This mutation is a conservative amino acid change and gives a slight bulkiness to the residue. However, the D3S5 domain forms the pore of the channel and the V1366 residue is highly conserved among vertebrate and invertebrate sodium channel alpha subunits and human calcium channel alpha subunits (Fig. 2). Therefore it is still possible that the mutation may critically affect the channel function. Apparently, functional studies are necessary to confirm the causative role of this channel mutation.

The mother (I-1) of the proband in family B is unaffected even if she had the mutation indicating its incomplete penetrance. The father in family B, who had a FS but not the mutation, would be a phenocopy. We recently reported a case of mosaicism in a family of SMEI and proposed that mosaicism may play roles in diverse phenotypes of members harboring identical mutations in some familial SMEI cases (Morimoto et al., 2006). It is also possible that mosaicism plays a role for the phenotype of mother (I-1) in family B. However, mosaicism may not be a player in determining the ultimate phenotype for the proband (II-1) in the family B because his mother has the mutation. Also in the family A, the V1366I mutation has been transmitted through members, and therefore mosaicism is not expected in patients II-3, II-4, III-3, III-5, and III-6. These results suggest that unidentified modifier(s) such as polymorphisms in other genes may be critical for ultimate phenotypes of the patients with the V1366I mutations in these families.

In addition to epileptic syndromes, two members from the family A showed psychiatric conditions that are panic disorder and Asperger syndrome. The DSM-IV (American Psychiatric Association, 1994) defines panic disorder as the spontaneous, unexpected occurrence of panic attacks followed by persistent concern, worry, and anxiety. Asperger

Please cite this article in press as: Osaka, H. et al., Patients with a sodium channel alpha 1 gene mutation show wide phenotypic variation, Epilepsy Res. (2007), doi:10.1016/j.eplepsyres.2007.03.018

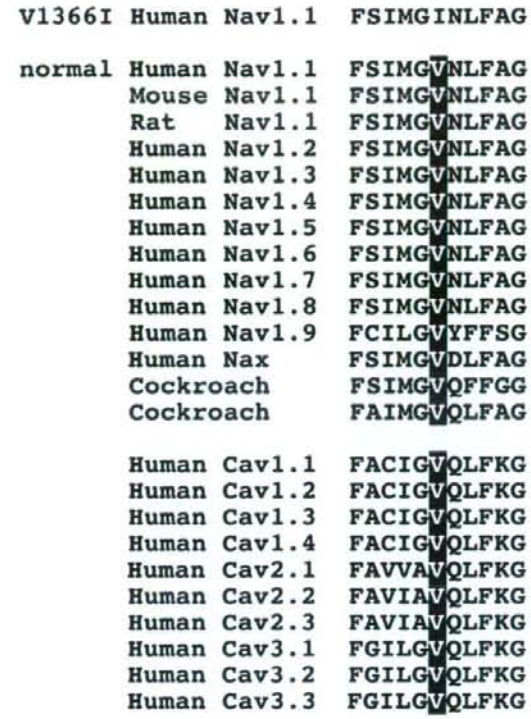

Figure 2 The valine residue for the c.4096G>A (V1366I) mutation is conserved among vertebrate and invertebrate sodium channel alpha subunits and human calcium channel alpha subunits. The valine residue corresponding to V1366 of human Nav1.1 is highlighted in black. Sources of sequences are as follows (notations refer to accession numbers): Human Nav1.1, NP_008851; mouse Nav1.1, NP_061203; rat Nav1.1, NP_110502; human Nav1.2, NP_001035232; human Nav1.3, NP_008853; human Nav1.4, NP_000325; human Nav1.5, NP_932173; human Nav1.6, NP_055006; human Nav1.7, NP_002968; human Nav1.8, NP_006505; human Nav1.9, NP_054858; human Nax, NP_002967; cockroach sodium channels, AAC47483 and AAK01090; human Cav1.1, NP_000060; human Cav1.2, NP_000719; human Cav1.3, NP_000711; human Cav1.4, NP_005174; human Cav2.1, NP_000059; human Cav2.2, NP_000709; human Cav2.3, NP_000712; human Cav3.1, NP_061496; human Cav3.2, NP_066921; human Cav3.3, NP_066919.

syndrome is one condition in the pervasive developmental disorders (autistic spectrum) and shares the common physiological problem with autism in an impairment of social interaction, but it is primarily distinguished from autism by the higher cognitive abilities and a more normal and timely development of language and communicative phrases. Twin and adoption studies showed strong genetic contribution on both panic disorder and autism spectrum (Piven and Palmer, 1999). Anxiety in autism patient is effectively treated with serotonin transporter inhibitors that are used for panic disorders (Kolevzon et al., 2006). This implies that these two distinct conditions may partially overlap in biological abnormality.

Considering the essential role of sodium channels in the CNS and the sensitivity of neuronal firing patterns to subtle mutations in these channels, SCN mutations may affect emotional and cognitive functions (Meisler et al., 2002). However, no autistic spectrum and other psychiatric illnesses had not been reported in families with FC plus, ICEGTC or SMEI. Weiss et al. (2003) sequenced *SCN1A* autism patients from Autism Genetic Research Exchange Families. Among 117 families tested, 5 missence mutations, R542Q, I1034T, F1038L, R1902C, were found in 6 patients. These mutations were not found in control tested. R542Q and F1038L mutations were shared by siblings. They hypothesized that, even though *SCN1A* mutations may not be major determinants of genetic abnormalities in autism, the combined effect of these mutations may predispose to these psychiatric diseases (Meisler and Kearney, 2005; Weiss et al., 2003).

The results described in this study may further support their proposal. Additional examination using model mouse, functional tests and population studies may contribute to the elucidations of molecular pathology of *SCN1A* mutations on epilepsy and psychiatric disorders.

References

Abou-Khalil, B., Ge, Q., Desai, R., Ryther, R., Bazyk, A., Bailey, R., Haines, J.L., Sutcliffe, J.S., George Jr., A.L., 2001. Partial and generalized epilepsy with febrile seizures plus and a novel *SCN1A* mutation. Neurology 57, 2265–2272.

Annesi, G., Gambardella, A., Carrideo, S., Incorpora, G., Labate, A., Pasqua, A.A., Civitelli, D., Polizzi, A., Annesi, F., Spadafora, P., et al., 2003. Two novel SCN1A missense mutations in generalized epilepsy with febrile seizures plus. Epilepsia 44, 1257–1258.

Bonanni, P., Malcarne, M., Moro, F., Veggiotti, P., Buti, D., Ferrari, A.R., Parrini, E., Mei, D., Volzone, A., Zara, F., et al., 2004. Generalized epilepsy with febrile seizures plus (GEFS$^+$): clinical spectrum in seven Italian families unrelated to *SCN1A*, *SCN1B*, and *GABRG2* gene mutations. Epilepsia 45, 149–158.

Ceulemans, B.P., Claes, L.R., Lagae, L.G., 2004. Clinical correlations of mutations in the *SCN1A* gene: from febrile seizures to severe myoclonic epilepsy in infancy. Pediatr. Neurol. 30, 236–243.

Escayg, A., Heils, A., MacDonald, B.T., Haug, K., Sander, T., Meisler, M.H., 2001. A novel *SCN1A* mutation associated with generalized epilepsy with febrile seizures plus and prevalence of variants in patients with epilepsy. Am. J. Hum. Genet. 68, 866–873.

Fujiwara, T., Sugawara, T., Mazaki-Miyazaki, E., Takahashi, Y., Fukushima, K., Watanabe, M., Hara, K., Morikawa, T., Yagi, K., Yamakawa, K., Inoue, Y., 2003. Mutations of sodium channel alpha subunit type 1 (SCN1A) in intractable childhood epilepsies with frequent generalized tonic–clonic seizures. Brain 126, 531–546.

Gerard, F., Pereira, S., Robaglia-Schlupp, A., Genton, P., Szepetowski, P., 2002. Clinical and genetic analysis of a new multigenerational pedigree with GEFS$^+$ (Generalized Epilepsy with Febrile Seizures Plus). Epilepsia 43, 581–586.

Goldin, A.L., 2001. Resurgence of sodium channel research. Annu. Rev. Physiol. 63, 871–894.

Ito, M., Nagafuji, H., Okazawa, H., Yamakawa, K., Sugawara, T., Mazaki-Miyazaki, E., Hirose, S., Fukuma, G., Mitsudome, A., Wada, K., Kaneko, S., 2002. Autosomal dominant epilepsy with febrile seizures plus with missense mutations of the (Na^+)-channel α1 subunit gene, *SCN1A*. Epilepsy Res. 48, 15–23.

Kolevzon, A., Mathewson, K.A., Hollander, E., 2006. Selective serotonin reuptake inhibitors in autism: a review of efficacy and tolerability. J. Clin. Psychiatry 67, 407–414.

Please cite this article in press as: Osaka, H. et al., Patients with a sodium channel alpha 1 gene mutation show wide phenotypic variation, Epilepsy Res. (2007), doi:10.1016/j.eplepsyres.2007.03.018